University of Alberta

Evaluation of the Re-Os Geochronometer in Organic-rich Mudrocks as a Method for Constraining the Absolute Ages of Neoproterozoic Glaciogenic Deposits

by

Brian Kendall

©

A thesis submitted to the Faculty of Graduate Studies and Research in partial fulfillment of the requirements for the degree of Master of Science

Department of Earth and Atmospheric Sciences

Edmonton, Alberta

Spring 2003

National Library of Canada
Acquisitions and Bibliographic Services
395 Wellington Street
Ottawa ON K1A 0N4
Canada

Bibliothèque nationale du Canada
Acquisitions et services bibliographiques
395, rue Wellington
Ottawa ON K1A 0N4
Canada

Your file Votre référence

Our file Notre référence

The author has granted a non-exclusive licence allowing the National Library of Canada to reproduce, loan, distribute or sell copies of this thesis in microform, paper or electronic formats.

L'auteur a accordé une licence non exclusive permettant à la Bibliothèque nationale du Canada de reproduire, prêter, distribuer ou vendre des copies de cette thèse sous la forme de microfiche/film, de reproduction sur papier ou sur format électronique.

The author retains ownership of the copyright in this thesis. Neither the thesis nor substantial extracts from it may be printed or otherwise reproduced without the author's permission.

L'auteur conserve la propriété du droit d'auteur qui protège cette thèse. Ni la thèse ni des extraits substantiels de celle-ci ne doivent être imprimés ou autrement reproduits sans son autorisation.

0-612-82295-8

Canada

University of Alberta

Library Release Form

Name of Author: Brian Stanley Kendall

Title of Thesis: Evaluation of the Re-Os Geochronometer in Organic-rich Mudrocks as a Method for Constraining the Absolute Ages of Neoproterozoic Glaciogenic Deposits

Degree: Master of Science

Year this Degree Granted: 2003

Permission is hereby granted to the University of Alberta Library to reproduce single copies of this thesis and to lend or sell such copies for private, scholarly or scientific research purposes only.

The author reserves all other publication and other rights in association with the copyright in the thesis, and except as herein before provided, neither the thesis nor any substantial portion thereof may be printed or otherwise reproduced in any material form whatever without the author's prior written permission.

Brian Kendall
Apartment #307B
14507 Miller Boulevard
Edmonton, Alberta, Canada
T5Y 3A8

January 20, 2003

University of Alberta

Faculty of Graduate Studies and Research

The undersigned certify that they have read, and recommend to the Faculty of Graduate Studies and Research for acceptance, a thesis entitled "Evaluation of the Re-Os Geochronometer in Organic-rich Mudrocks as a Method for Constraining the Absolute Ages of Neoproterozoic Glaciogenic Deposits" submitted by Brian Stanley Kendall in partial fulfillment of the requirements for the degree of Master of Science.

Dr. Robert Creaser
Supervisor

Dr. Thomas Chacko
Committee Chair/Examiner

Martyn Unsworth
Dr. Martyn Unsworth
Committee Member

13 Jan 2003
Date

ABSTRACT

Precise ^{187}Re-^{187}Os ages of 620.8 ± 8.1 Ma and 607.6 ± 8.3 Ma were obtained with inverse aqua regia and CrO_3-H_2SO_4 dissolution techniques, respectively, for carbonaceous, sulfidic slates of the Old Fort Point Formation (OFP), Windermere Supergroup. The CrO_3-H_2SO_4 method provides the most accurate determination of the depositional age and $^{187}Os/^{188}Os$ isotopic ratio (0.63 ± 0.05) of Neoproterozoic seawater. The OFP is believed to be the deep-water facies equivalent of carbonates that cap the Mount Vreeland and Ice Brook diamictites in the Canadian Cordillera. A minimum age constraint of ~ 608 Ma is therefore inferred for the second Windermere glaciation which correlates it with other Lower Marinoan glaciogenic deposits. A geologically meaningless age (471 ± 11 Ma) was obtained for more metamorphosed slates of the stratigraphically higher Upper Miette Group. This suggests the Re-Os geochronometer may not be applicable to organic-rich mudrocks metamorphosed higher than lower-greenschist (-chlorite) grade.

ACKNOWLEDGEMENTS

The research for this M.Sc. project was supported by a NSERC research grant to Dr. Robert Creaser. I wish to thank both Dr. Creaser and Dr. Tom Chacko for the helpful discussions involving this project. Dr. Gerry Ross of the Geological Survey of Canada (Calgary) assisted in identifying sampling localities and also provided stable isotope data as well as insights on the geology of the Windermere Supergroup. David Selby is thanked for answering my inexhaustible store of questions on the analytical techniques used for the Re-Os system. Stacey Hagen provided invaluable aid with mass spectrometer work. I also wish to extend my appreciation to my family and Kimberly Reid for their support.

TABLE OF CONTENTS

Introduction.....1

Geology.....7
- Old Fort Point Formation.....7
- Upper Miette Group.....13
- Deformation and Metamorphism in the Rocky Mountain Belt... 14

Analytical Methods.....16
- Sampling Details.....16
- Re-Os Analysis with Conventional Inverse Aqua Regia Dissolution.....19
- Re-Os Analysis with CrO_3-H_2SO_4 Dissolution.....22
- Negative Thermal Ionization Mass Spectrometry.....24

Results.....26
- Re and Os Concentrations and Isotope Variations.....26
- Re-Os Age Determinations.....31

Discussion.....38
- Re-Os Systematics of the OFP: Implications for Future Re-Os Dating of ORMs.....38
- Implications for the Neoproterozoic Glaciations.....44
- $^{187}Os/^{188}Os$ Isotopic Composition of ~ 608 Ma Neoproterozoic Seawater.....51
- Re-Os Isotope Systematics and Metamorphism.....56

Conclusions.....63

References.....66

Appendix One: Sample Details.....83

LIST OF TABLES

Table 1: Re and Os concentrations and isotope data for inverse aqua regia and CrO_3-H_2SO_4 analyses of the OFP slates.....27

Table 2: Re and Os concentrations and isotope data for inverse aqua regia analyses of the UMG slates.....28

Table 3: Summary of known geochronological age constraints on Marinoan glacial deposits.....46

LIST OF FIGURES

Figure 1: Distribution of the Windermere Supergroup in A) western North America and B) within the regional geological setting of the southeastern Canadian Cordillera.....8

Figure 2: Stratigraphic columns for the Windermere Supergroup in the Canadian Cordillera showing the inferred correlations between the diamictites (Ice Brook and Mount Vreeland Formations) and cap carbonates (Teepee Dolomite and basal Framstead Formation) of the second Windermere glaciation and their relationship to the OFP.....11

Figure 3: Re-Os isochron diagrams for OFP samples analyzed by conventional inverse aqua regia dissolution.....32

Figure 4: Re-Os isochron diagrams for OFP samples analyzed by CrO_3-H_2SO_4 dissolution.....34

Figure 5: Comparative Re-Os isochron diagrams showing A) inverse aqua regia and B) CrO_3-H_2SO_4 regressions of one analysis of every sample except BK-01-014A.....36

Figure 6: Re-Os isochron diagrams for UMG samples analyzed by conventional inverse aqua regia dissolution.....37

Figure 7: Initial $^{187}Os/^{188}Os$ isotopic ratios (I_{Os}) for each OFP sample at 608 Ma.....43

Figure 8: Compositions of the known Os sources to present-day seawater.....53

Figure 9: $\delta^{13}C_{org}$ isotope profile of the Liassic black shale series (Swiss Alps) showing progressive enrichment in organic carbon isotopic composition during prograde metamorphism....60

ABBREVIATIONS

$I_{Os(t)}$	Initial $^{187}Os/^{188}Os$ isotopic composition at t Ma
Ma	Mega anos (million years)
MSWD	Mean square of weighted deviates
NTIMS	Negative thermal ionization mass spectrometry
OFP	Old Fort Point Formation
ORM	Organic-rich mudrock
ppb	Parts per billion
ppt	Parts per trillion
TOC	Total organic content
UMG	Upper Miette Group

INTRODUCTION

Neoproterozoic glacial deposits are found on every continent and differ from their Phanerozoic counterparts in their enigmatic associations with warm-water lithological indicators such as carbonates. Paleomagnetic studies have confirmed this apparent climatological paradox by demonstrating a low-latitude origin for several of these diamictites (see Evans, 2000 for a review). During the last decade, a plethora of chemostratigraphic, radiometric, petrological, and climate-modelling studies have been carried out to understand the mechanisms that could have caused the formation of both low latitude and altitude ice sheets and the large negative $\delta^{13}C$ isotopic excursions present in the cap carbonates that overlie Neoproterozoic glacial deposits worldwide. This has led to the development of several models to explain these unusual features; of these, the Snowball Earth theory (Kirschvink, 1992; Hoffman et al., 1998a, b; Hoffman and Schrag, 2000, 2002) and, to a lesser degree, the high orbital obliquity hypothesis (Williams, 1975, 1993, 1998; Williams et al., 1998; Williams and Schmidt, 2000) have recently been the subject of considerable debate and scrutiny. The Snowball Earth theory proposes that concentration of relatively small Neoproterozoic continents around middle to low latitudes (caused by the breakup of the supercontinent Rodinia) led to CO_2 drawdown from the atmosphere (through intensive silicate weathering) and a higher planetary albedo; together this caused the buildup of polar sea ice. Although the trigger

effect for each Snowball event is not yet understood (an overdependence on methane as a greenhouse gas has been recently suggested; Pavlov et al., 2000; Halverson et al., 2002; Schrag et al., 2002), the buildup of highly reflective snow and ice eventually led to a runaway albedo effect that encased the planet in ice and nearly terminated the hydrologic cycle. Each individual ice age may have lasted up to 30 Ma and only ended after a catastrophic buildup of CO_2 from volcanism resulted in the rapid melting of ice sheets and, subsequently, an exceptionally severe greenhouse effect. More moderate variations of this theory have also been suggested (e.g., ice-free equatorial water masses in an otherwise frozen Earth; Hyde et al., 2000; Crowley et al., 2001). In contrast, the high orbital obliquity hypothesis suggests that an increased obliquity of the ecliptic (54°) for the Earth during Precambrian times confined the development of Neoproterozoic ice sheets to latitudes less than 40° north or south of the equator (at high obliquities, the polar regions receive more solar insolation than the tropics). Such a scenario may have led to the development of diachronous glaciations as the continents moved through low latitudes. These two contrasting models can be directly tested using paleomagnetic or absolute age determinations of the Neoproterozoic glaciogenic deposits (Evans, 2000). However, a high paleomagnetic pole position that could discount the high orbital obliquity hypothesis has not yet been found. If instead synchroneity could be demonstrated for the diamictites, this would support a Snowball Earth model. However, the

extent (e.g., global or nonglobal), timing, and duration of the Neoproterozoic glaciations, as well as the number of ice ages, remain largely unconstrained. This problem results from a paucity of suitable igneous rocks that are temporally and spatially related to Neoproterozoic glaciogenic deposits and are amenable to radiometric dating methods. As a result, only a few of the diamictites have reliable absolute age constraints (usually provided by U-Pb zircon dates of intercalated ash beds) and these are not sufficient to allow a detailed assessment of the Snowball Earth theory.

As a result of recent technical advances, the application of the ^{187}Re (rhenium) – ^{187}Os (osmium) radioisotope system to organic-rich mudrocks (ORMs) has established this system as the only long-lived geochronometer capable of providing a precise depositional age for clastic sedimentary rocks (Ravizza and Turekian, 1989; Cohen et al., 1999; Singh et al., 1999; Creaser et al., 2002; Selby and Creaser, 2002). In some cases, ORMs stratigraphically underlie Neoproterozoic glaciogenic deposits (e.g., the Aralka Formation of the Amadeus Basin in Australia; Schaefer and Burgess, 2001). In other cases, ORMs overlie, or are facies equivalents of, carbonates that typically cap the diamictites (e.g., the Tindelpina Shale of the Adelaide Geosyncline in Australia; McKirdy et al., 2001). Thus, the Re-Os geochronometer has the potential to provide maximum or minimum absolute age constraints on the Neoproterozoic glacial deposits and can therefore also aid in their

worldwide correlation. The present study evaluates the suitability of the Re-Os geochronometer for this purpose by focusing on the carbonaceous, sulfidic slates of the Old Fort Point Formation, a widespread fine-grained marker unit within the Windermere Supergroup of the southeastern Canadian Cordillera (Ross and Murphy, 1988). The Old Fort Point Formation has previously been interpreted as the deep-water facies equivalent to the cap carbonates of the second Windermere glaciation (represented in the Canadian Cordillera by the glaciogenic Mount Vreeland and Ice Brook Formations of northeastern British Columbia and the Mackenzie Mountains, N. W. T., respectively; Ross, 1991a; Ross et al., 1995).

The present study also investigates the effect of two processes that would be detrimental to the ability of the Re-Os geochronometer to provide a precise depositional age for a Neoproterozoic (or any other age) ORM sample suite: detrital contamination and metamorphism. Within these sedimentary rocks, most of the Re and Os are associated with organic matter and are dominantly hydrogenous in origin since they are sequestered from seawater during, or very soon after, sediment deposition (Ravizza and Turekian, 1989; Ravizza et al., 1991; Ravizza and Turekian, 1992; Ravizza and Esser, 1993; Cohen et al., 1999; Martin et al., 2000; Peucker-Ehrenbrink and Hannigan, 2000; Pierson-Wickmann et al., 2000, 2002; Jaffe et al., 2002; Selby and Creaser, 2002). However, Selby and Creaser (2002) showed that a small, but significant, fraction of non-

hydrogenous Re and Os is also present in ORMs of the Late Devonian Exshaw Formation (Western Canada Sedimentary Basin). This detrital component can result in erroneous determinations of the Re-Os age and initial $^{187}Os/^{188}Os$ isotopic ratio (and hence the contemporaneous seawater Os isotopic composition) of an ORM sample suite analyzed with conventional inverse aqua regia dissolution (i.e., employing concentrated solutions of HCl and HNO_3 in a 1:2 ratio). The present study considers the effects of such detrital contamination on ORMs such as the Old Fort Point Formation slates that contain low (< 1%) total organic content. By comparing Re-Os data obtained using a CrO_3-H_2SO_4 digestion technique (Selby and Creaser, 2002) and inverse aqua regia (Creaser et al., 2002), I show that the Old Fort Point Formation slates contain a significant radiogenic detrital Re and Os component that is mixed with hydrogenous Re and Os. This provides further support to the CrO_3-H_2SO_4 dissolution method as superior to the inverse aqua regia technique for Re-Os dating studies on ORM horizons.

The response of the Re-Os radioisotope system in ORMs to prograde metamorphism remains unknown. Creaser et al. (2002) recently demonstrated that the Re-Os isotope systematics of the organic-rich Exshaw Formation did not show any evidence of disturbance by hydrocarbon maturation processes. Ripley et al. (2001a, b) analyzed physically separated organic matter from carbonaceous argillites of the Virginia Formation (northeastern Minnesota) and presented evidence of

open-system Re-Os behavior caused by metasomatic processes during weak contact metamorphism. However, Selby and Creaser (2002) demonstrated, using the ORMs from the Exshaw Formation, that the HF-BF_3 organic matter extraction procedure employed by Ripley et al. disturbs the Re-Os systematics of ORM samples by preferentially leaching Re. The apparently disturbed Re-Os systematics of the weakly metamorphosed Virginia Formation argillites is thus likely analytical, rather than geological, in nature. The present study attempts to provide a first look at the systematics of the Re-Os geochronometer in ORMs subjected to lower greenschist-grade metamorphism. Using the Old Fort Point Formation slates, it is demonstrated for the first time that the Re-Os system remains undisturbed during low-chlorite grade metamorphism. However, the present study also shows that middle-chlorite grade carbonaceous, sulfidic slates from the Upper Miette Group of the Windermere Supergroup (northern Selwyn Range) contain evidence of open-system Re-Os behavior that resulted in the determination of a geologically meaningless age that is intermediate between the true depositional and metamorphic ages.

GEOLOGY

Old Fort Point Formation

The grit division of the Windermere Supergroup in the southeastern Canadian Cordillera is composed of thick sequences containing turbiditic, immature, feldspathic sandstones, granule conglomerates, and pelites (Ross et al., 1989; Ross et al., 1995). The nomenclature for these clastic sedimentary rocks is varied and includes the middle Miette Group in the western Main Ranges of the Rocky Mountains; the Kaza Group in the northern Cariboo Mountains; and the Horsethief Creek Group in the Monashee, northern Purcell, and Selkirk Mountains (e.g., Campbell et al., 1973; Pell and Simony, 1987; Ross and Murphy, 1988). Along with most of the Windermere Supergroup in the southeastern Canadian Cordillera, the grits were deposited in a northwest-trending longitudinal, basinal, turbidite system (Ross et al., 1989; Ross, 1991b) either along a west-facing passive margin (Ross, 1991b; Ross et al., 1995) or within a 2500 km long intracontinental rift system (Colpron et al., 2002). The middle and upper sections of the grits are separated by a widespread, fine-grained marker unit termed the Old Fort Point Formation (OFP; Charlesworth et al., 1967). This marker unit is exposed over an area of 35,000 km^2 throughout southeastern British Columbia and southwestern Alberta (figure 1). The OFP is composed of a fining-upward sequence of variable thickness (up to 300 m) containing siltstone,

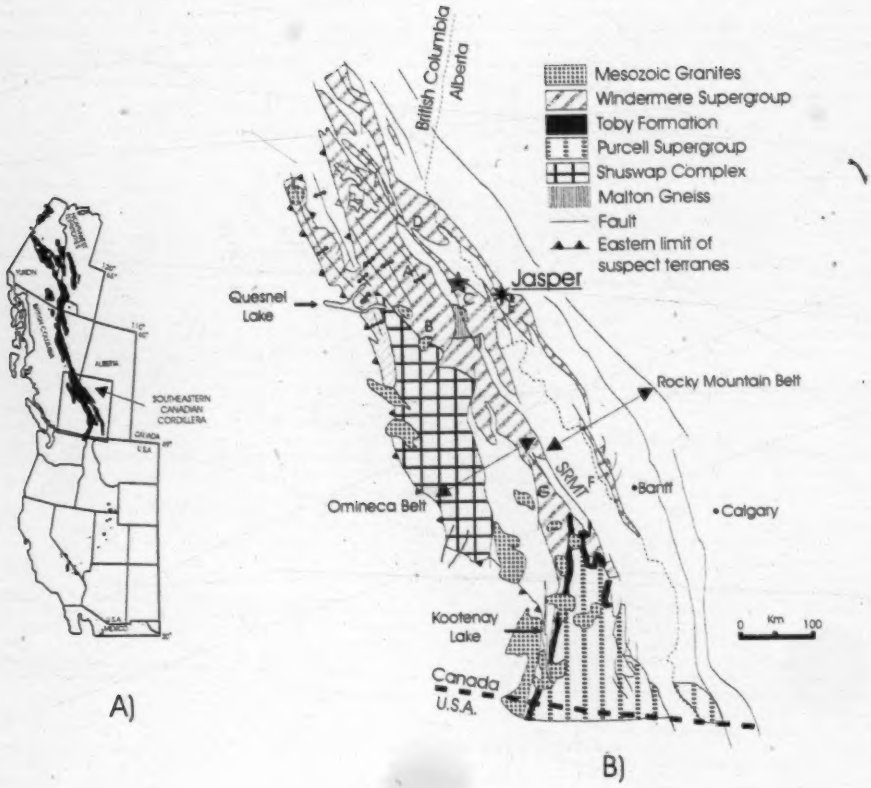

FIGURE 1: Distribution of the Windermere Supergroup in A) western North America and B) within the regional geological setting of the southeastern Canadian Cordillera. The known localities of the OFP (A-G) and the sampling localities for this study (✷ - OFP; ★ - UMG) are also shown. SRMT = Southern Rocky Mountain Trench. Modified after Ross et al. (1995).

rhythmic marble-pelite, and sulfidic, carbonaceous pelite. The fine-grained nature of the OFP represents the development of anoxic conditions and the termination of clastic sediment deposition as a result of an eustatic sea-level rise throughout the Windermere basin (Ross and Murphy, 1988). The carbonaceous interval of the OFP records the highstand conditions produced by maximum flooding of the Windermere basin. From west to east, the OFP undergoes a change from anoxic to oxic facies which corresponds to a paleogeographic transition from the Windermere basin floor to the upper continental slope (Ross and Murphy, 1988; Ross et al., 1989). This is reflected by a gradual decrease in thickness of the carbonaceous interval from approximately 20 m thick in the Cariboo Mountains to nearly 4 m thick at Geikie-Siding (14 km west of Jasper). In the vicinity of Jasper, this interval is replaced by vari-colored slates (Charlesworth et al., 1967; Ross and Murphy, 1988; Ross et al., 1989).

The carbonaceous interval of the OFP is capped by argillaceous and arenaceous limestone breccia (Ross et al., 1995). These locally contain carbonate clasts with pseudomorphic calcite (originally aragonite) crystal rosette and tepee structures similar to those present within the fine-grained, thinly-laminated Teepee Dolomite (cap carbonate of the glaciogenic Ice Brook Formation) in the Mackenzie Mountains (Aitken, 1991a; Ross, 1991a; Ross et al., 1995). These features are also found within the carbonate clasts from the carbonaceous pelites (basal

Framstead Formation) overlying the cap carbonate of the glaciogenic Mount Vreeland Formation (Monkman Pass area of northeastern British Columbia; Ross, 1991a; Ross et al., 1995; McMechan, 2000). In this case, the carbonate clasts are interpreted as olistoliths derived from cap carbonates deposited to the east on the Windermere continental shelf (McMechan, 2000). In addition, $\delta^{13}C_{org}$ values as low as -32‰ characterize both the OFP carbonaceous interval and the limestone clasts from the overlying breccia; strongly negative $\delta^{13}C_{carb}$ values are also present within the latter (G. M. Ross, personal communication, 2002). Similarly, negative $\delta^{13}C$ values have been found in the carbonate olistoliths from the basal Framstead Formation (G. M. Ross, personal communication, 2002) and within the Teepee Dolomite (Narbonne et al., 1994; Kaufman et al., 1997; James et al., 2001). These lithological and chemostratigraphic similarities strongly support the correlation of the OFP with the cap carbonates of the Mount Vreeland and Ice Brook diamictites (figure 2) and is consistent with the interpretation that the OFP represents the product of a post-glacial sea-level rise (Ross, 1991a; Ross et al., 1995). Together, the Mount Vreeland and Ice Brook diamictites represent a second Windermere ice age (McMechan, 1990; Hein and McMechan, 1994) that is distinct from the older Windermere glaciogenic deposits of the Toby Formation (southernmost Canadian Cordillera and the northwestern United States; Aalto, 1971) and Rapitan Group (Mackenzie Mountains; Young, 1976). Within the southern

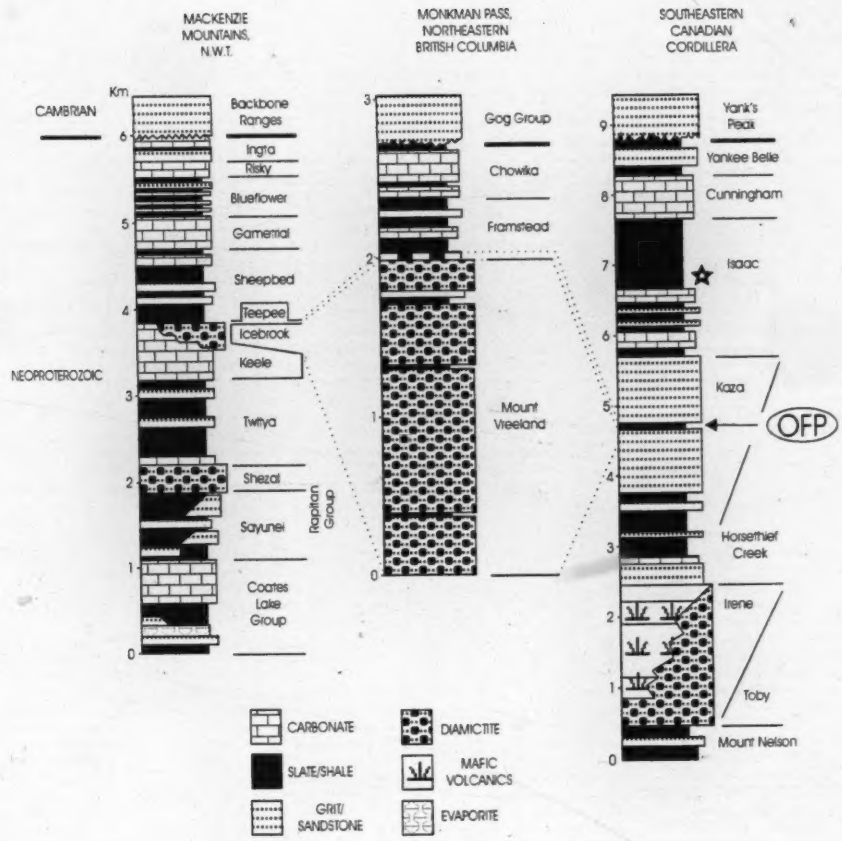

FIGURE 2: Stratigraphic columns for the Windermere Supergroup in the Canadian Cordillera showing the inferred correlations between the diamictites (Ice Brook and Mount Vreeland Formations) and cap carbonates (Teepee Dolomite and basal Framstead Formation) of the second Windermere glaciation and their relationship to the OFP. The lithological nomenclature for the southeastern Canadian Cordillera is based on strataigraphic sections from the Cariboo and Purcell Mountains. The equivalent strata in the southern Rocky Mountains are the Lower (Lower Kaza and Horsethief Creek Groups), Middle (Middle to Upper Kaza and Horsethief Creek Groups), and Upper (Isaac, Cunningham, and Yankee Belle Formations) Miette Group (e.g., Campbell et al., 1973; Pell and Simony, 1987; Ross and Murphy, 1988). Sampling location for the UMG in this study is shown by the star. Modified after Ross et al. (1995).

Canadian Cordillera, there are no diamictites corresponding to the second Windermere glaciation because of the distal offshore paleogeographic position within the Windermere basin. The eustatic sea-level rise recorded by the OFP thus represents (indirectly) the only record of this glaciation in the southern Canadian Cordillera. However, field studies have demonstrated an abrupt southwest lateral facies change of the Mount Vreeland diamictites into turbiditic grits and pelites similar to those of the middle Miette Group (McMechan, 1987, 1990; Hein and McMechan, 1994; McMechan and Thompson, 1995; Ross et al., 1995; McMechan, 2000). This is also reflected by the position of the coarsest Windermere turbiditic grits directly beneath the OFP (G. M. Ross, personal communication, 2002).

The maximum age of the Windermere Supergroup is ~ 762-728 Ma (based on U-Pb zircon and Sm-Nd dates from granitic and volcanic rocks that unconformably underlie the Windermere or intrude its basal succession; Ross et al., 1995 and references therein; Ross and Villeneuve, 1997). These dates provide relatively good age constraints on the timing of the first Windermere glaciation and correlate it with other Sturtian (~ 740-720 Ma; Evans, 2000) glaciogenic deposits worldwide. In contrast, absolute age constraints for the timing of the Ice Brook – Mount Vreeland ice age are poor. Maximum age constraints do not exist for these diamictites above the stratigraphic level of the Rapitan Group and Toby Formation glacial deposits. A minimum age is provided by a U-Pb

zircon date of 569.6 ± 5.3 Ma from Hamill Group volcanic rocks that unconformably overlie the Windermere Supergroup (Colpron et al., 2002). Thus, Re-Os dating of the OFP represents an excellent opportunity to provide a strong minimum age constraint on the timing of the second Windermere glaciation. The Ice Brook and Mount Vreeland diamictites have previously been considered as Marinoan in age (Aitken, 1991b; Ross et al., 1995). Current geochronological constraints suggest that at least two distinct Marinoan ice ages occurred at ~ 620-600 Ma and ~ 580-570 Ma (Evans, 2000 and references therein).

Upper Miette Group

In the northern Selwyn Range, the Miette Group has been described in detail by McDonough and Simony (1986, 1988) and is briefly summarized here. The lower Miette Group is at least 850 m thick and is composed of dark grey and black pelites interbedded with quartzite and occasionally thin, fine-grained, black limestone. As is the case elsewhere in the southeastern Canadian Cordillera, the overlying middle Miette Group consists of two thick (2300-2600 m) successions of coarse, immature, feldspathic and conglomeratic grit interbedded with green, brown, and rare black pelite. These two grit successions are separated by a fine-grained triad marker unit that is correlative with the OFP.

The Upper Miette Group (UMG) is a continental slope succession (correlative with the Isaac Formation; Campbell et al., 1973; McDonough

and Simony, 1988) that consists of at least 600 m of dark-colored calcareous pelites, limestones and subordinate grit that can be subdivided into three units. The basal 330 m is composed of abundant dark brown, dark grey and black sulfidic, calcareous pelites. Minor thin sandstone interbeds dominate near the base while limestone interbeds become more abundant near the top. Approximately 300 m from the base of the UMG is a 1.5 m thick conglomerate bed containing limestone and quartz clasts cemented with calcite. The middle UMG is composed of a 200 m thick black limestone succession. The 1.5 m conglomerate bed and the middle UMG are likely correlative with the two deep-water allodapic carbonate marker units of the Isaac Formation (IC1 and IC2 of Ross et al., 1995) that are present in the Cariboo Mountains and throughout the southern Canadian Cordillera. Ross et al. (1995) interpreted these units as recording carbonate platform progradation caused by eustatic sea-level fall. The top of the UMG is dominantly composed of at least 70 m of brown and black sulfidic, calcareous pelite with minor thin interbeds of feldspathic and conglomeratic grit. The upper contact of the UMG is not exposed in the northern Selwyn Range.

Deformation and Metamorphism in the Rocky Mountain Belt

The Windermere Supergroup was affected by the widespread deformation, metamorphism, uplift, and granitic magmatism associated with the collision of two composite superterranes with the ancient western

margin of North America during Jurassic to Eocene times (Monger and Price, 1979; Monger et al., 1982). The paleo-continental margin was first deformed during obduction of the Intermontane superterrane during Mid-Jurassic to Mid-Cretaceous times (Price, 1994); peak metamorphic conditions (to the upper amphibolite facies) were reached in the Mid-Jurassic within the Omineca Crystalline Belt (Greenwood et al., 1991; see figure 1). This tectonic belt represents the suture between the accreted Intermontane Belt and the western North American paleo-miogeocline. A second deformational event, responsible for the uplift of the Rocky Mountains, was related to the obduction of the Insular superterrane and affected the Canadian Cordillera during the Mid-Cretaceous to Mid-Eocene (Price, 1994). Metamorphism within the Rocky Mountain Fold and Thrust Belt generally does not exceed lower greenschist facies (chlorite and biotite grade) and is considered to be largely the result of regional burial metamorphism (Greenwood et al., 1991). However, Charlesworth et al. (1967) demonstrated that cleavage in middle Miette Group rocks near Jasper is symmetrical about fold axial surfaces and that metamorphic platy minerals (muscovite and chlorite) are related to cleavage. Together, this suggests that metamorphism also occurred penecontemporaneously with deformation. Near Jasper in the western Main Ranges, middle Miette Group strata (including the OFP) have reached the low-chlorite metamorphic grade (as indicated by the presence of quartz-albite-chlorite-muscovite mineral assemblages; Charlesworth et

al., 1967). A general westward increase in metamorphic grade is indicated by the appearance of chloritoid-bearing phyllites (upper-chlorite grade) in the northern Selwyn Range (McDonough and Simony, 1988) and biotite schists (biotite grade) near Tete Juane Cache (Charlesworth et al., 1967). In addition, Charlesworth et al. (1967) found a general westward decrease in K-Ar dates (from ~ 400 Ma at Jasper to 69 Ma near Mount Robson, British Columbia) for whole-rock samples of middle Miette slates; this further suggests increasing metamorphic grades in this direction. This well-defined east-to-west increase in metamorphic grade through the Rocky Mountain Belt allows a first look at the response of the Re-Os radioisotope system in ORMs to prograde metamorphism through a comparison of the Re-Os systematics of the low-chlorite grade OFP and middle-chlorite grade UMG carbonaceous slates.

ANALYTICAL METHODS

Sampling Details

Outcrop samples were collected for Re-Os analysis from the carbonaceous, sulfidic slates of the OFP and UMG at Geikie-Siding, Alberta and within the northern Selwyn Range in British Columbia, respectively, during June 2001. The OFP slates contain up to 0.5% total organic content (TOC) and have nearly pristine (i.e., depositional) $\delta^{13}C_{org}$ values of -32‰ to -28‰ while the UMG slates are more enriched in

organic carbon (~ 1.8 to 2.1% TOC) and have less negative (but also likely near-pristine) $\delta^{13}C_{org}$ values of -29‰ to -25‰ (G. M. Ross, personal communication, 2002). The OFP carbonaceous interval at Geikie-Siding represents the least metamorphosed examples of these ORMs and thus this sampling locality provides the best opportunity for determining a precise Re-Os depositional age. The UMG slates selected for Re-Os analysis in the present study occur only a few kilometers northeast of the first occurrences of the chloritoid-bearing Miette Group phyllites described by McDonough and Simony (1988) and are thus considered to be of middle-chlorite grade.

Sampling involved the collection of large (at least 5 cm thick), fresh (i.e., containing unweathered pyrite with a metallic brass-yellow color) whole-rock ORM samples over a stratigraphic interval of ~ 50 cm from both localities. The selection of unweathered samples is especially important because a significant fraction of the initial Re, Os, and organic carbon budgets in ORMs are lost during weathering processes (Peucker-Ehrenbrink and Hannigan, 2000; Jaffe et al., 2002; Pierson-Wickmann et al., 2002).

Fresh material was extracted from the core of each sample and crushed for use in Re-Os analyses; the crushed sample mass ranged from 85 g to 310 g. Whole-rock samples were cut into cubes with a diamond saw blade to remove weathered material. These sample cubes were then ground on a diamond plate to remove the cutting marks. After wrapping

heavily in plastic, each rock cube was broken into small chips using a sledgehammer. Extreme care was taken to make sure no physical contact occurred between the sledgehammer and the sample cubes since trace Re and Os in the metal of the sledgehammer can potentially contaminate the samples. Using an automatic agate mill, the rock chips of each sample were crushed to fine powder. Cleaning of the mortar and pestle with ethanol and silica was done between samples to avoid cross-contamination.

Re and Os isotope analyses were carried out at the Radiogenic Isotope Facility of the Department of Earth and Atmospheric Sciences, University of Alberta. Among the facilities used are a class 100 clean room tracer isotope laboratory (equipped with class 10 workstations) and a mass spectrometer laboratory. The isotope dilution method was employed to determine the concentrations and isotopic compositions of ORM samples analyzed by negative thermal ionization mass spectrometry (NTIMS; Creaser et al., 1991; Völkening et al., 1991). Two digestion mediums, both employing the Carius tube method (modified after Shirey and Walker, 1995), were used in the extraction, separation, and purification of Re and Os from whole-rock powdered samples: conventional inverse aqua regia (slightly modified after Creaser et al., 2002) and selective dissolution of organic matter with a CrO_3-H_2SO_4 solution (after Selby and Creaser, 2002). The inverse aqua regia procedure dissolves both the non-hydrogenous (i.e., detrital and

meteoritic particulate contributions) and hydrogenous (i.e., seawater) Re and Os fractions of ORMs. In contrast, the CrO_3-H_2SO_4 dissolution technique excludes the non-hydrogenous component (although an undissolved extraterrestrial component from hydrocarbons, sulfides, and other Re- and Os-rich phases in meteorites and cosmic dust would likely be included; Selby and Creaser, 2002). Both procedures were used in the analysis of the OFP slates for the purpose of assessing the detrital Re and Os budget in these low-TOC ORMs. Only the inverse aqua regia method was applied to the UMG slates as these were analyzed to assess the response of the Re-Os radioisotope system to middle-chlorite grade metamorphism.

Re-Os Analysis with Conventional Inverse Aqua Regia Dissolution

For each sample, 1.15-1.25 g of accurately weighed whole-rock powder was added to a Carius tube (a thick-walled tube made of borosilicate glass). A known amount of a calibrated (using standard solutions prepared from 99.999% pure Re metal and 99.999% metal-based ammonium hexachlorosmate; Selby and Creaser, 2001) tracer solution containing isotopically-enriched ^{185}Re and ^{190}Os in 6N HCl was added to each sample. The tubes were then placed within a frozen slurry of dry ice and methanol. Inverse aqua regia was formed by dissolving the sample and spike in a 1:2 acid mixture containing 3 mL of 12N HCl and 6 mL of 16N HNO_3. The HNO_3 was added after the HCl – spike solution

had frozen. The tubes were then sealed with an oxygen – propane flame, loaded into stainless steel jackets, and heated for 48 hours at a temperature of 240°C. This allowed complete equilibration to occur between the sample and spike by ensuring that all Re and Os are digested from the matrix of each whole-rock powdered sample. Selby and Creaser (2002) found that the residue (primarily quartz and feldspar) left behind after digestion of Exshaw Formation ORMs (containing typically 2-4% TOC) by this method accounted for < 50% of the original whole-rock powders used.

The subsequent Os solvent extraction and microdistillation procedures are modified after those of Cohen and Waters (1996) and Birck et al. (1997). Following digestion of the samples and subsequent cooling to room temperature, each tube was frozen in liquid nitrogen to avoid any loss of volatile Os during the unsealing process. Upon opening of the tubes, 3.5 mL of chilled HPLC-grade CCl_4 was added to each tube. The tubes were allowed to thaw before their solutions were transferred to polypropylene 50 mL centrifuge vials that were then placed in a ~ 25°C water bath for 15 minutes. The vials were shaken for a minute and centrifuged to separate the CCl_4 (Os-bearing fraction) from the inverse aqua regia (Re-bearing fraction) solutions. This was followed by CCl_4 extraction and removal to 22 mL glass vials containing 3 mL of 9N HBr. These two previous steps (centrifuging and extraction) were repeated two more times with two further 3.5 mL portions of CCl_4. The CCl_4-HBr

solutions were sealed with Teflon-lined membrane caps and heated at ~ 60°C on a hotplate for a minimum of 12 hours to back-extract the Os from the CCl_4 into the HBr.

Following the Os back-extraction, the CCl_4 was discarded to waste. The HBr-Os solutions were transferred to watchglasses covered with PFA Teflon tape, dried down to ~ 30 µL size, transferred onto the Teflon-lined membrane caps, and dried down in HEPA filtered air at ~ 60°C on a hotplate. A microdistillation procedure was then used to purify the Os fractions. Os was first oxidized with 30 µL of a CrO_3-H_2SO_4 solution (containing 0.2 g of CrO_3 per 1 mL of 7N H_2SO_4) and then reduced with 20 µL of 9N HBr. This was accomplished using inverted, sealed, 3 mL tristar vials (PFA conical Teflon vials) placed onto a temperature-regulated heating block (T = 80°C) for ~ 3 hours with the HBr held in the apex of the vials. The resulting Os-HBr solutions were dried down on the heating block under a N_2 gas atmosphere at a temperature of 60°C for ~ 2.5 hours.

The inverse aqua regia solutions were dried down in disposable Polymethylpentene (PMP) beakers on a hotplate at ~ 80°C. The precipitates were dissolved for ~ 2 hours in 3 mL of 0.2N HNO_3 at room temperature and then heated at ~ 60°C on a hotplate for 10 minutes. The solutions were centrifuged for 10 minutes to gravitationally separate any residue. The purification of Re was carried out through anion exchange chromatography using disposable 1 mL LDPE columns, quartz wool

plugs, and Eichrom 1X8 100-200 mesh anion resin in a procedure modified after that of Morgan et al. (1991). The columns were first cleaned with 4 mL of 8N HNO_3 and then equilibrated with 4 mL of 0.2N HNO_3. The inverse aqua regia solutions were loaded into the columns and washed with four 0.25 mL portions of 0.2N HNO_3, two 1 mL portions each of 0.2N HNO_3 and 0.2N HCl, and finally 2 mL of 6N HNO_3. Using PMP beakers, 4 mL of Re was collected in 6N HNO_3 and dried down overnight at ~ 60°C on a hot plate in HEPA filtered air.

Re-Os Analysis with CrO_3-H_2SO_4 Dissolution

The selective dissolution of organic matter from whole-rock powdered samples was accomplished by digestion with a CrO_3-H_2SO_4 solution (containing 0.2 g of CrO_3 per 1 mL of 4N H_2SO_4; for details, see Selby and Creaser, 2002). As in the inverse aqua regia method, 1.15-1.30 g of accurately weighed whole-rock powder was added to a Carius tube, spiked, and placed into a methanol – dry ice slurry after which 8 mL of CrO_3-H_2SO_4 solution was added. The samples were again sealed and heated at 240°C for 48 hours and then cooled to room temperature. The residue left behind following CrO_3-H_2SO_4 dissolution accounted for nearly all of the Exshaw Formation samples used (i.e., > 90-95%) and consisted largely of quartz, feldspar, and muscovite as well as minor amounts of other minerals (e.g., precipitation products such as calcite, dolomite, and evaporite minerals) (Selby and Creaser,

2002). The CrO_3-H_2SO_4 method therefore digests much less of the rock matrix than the conventional inverse aqua regia procedure. The extraction and separation of the Os fraction from the dissolved organic matter was accomplished using the Os solvent extraction and microdistillation procedures as described above for the inverse aqua regia method.

For the anion exchange chromatography and single bead anion extraction procedures, 1 mL of the separated CrO_3-H_2SO_4 (Re-bearing fraction) solutions was used. Because Cr^{6+} introduces additional complications for anion exchange chromatography, a procedure modified from that of conventional inverse aqua regia is used for the purification of Re. The 1 mL solutions were mixed with 4 mL of H_2SO_3 to reduce the oxidation state of the chromium from +6 to +3. The solutions were then dried down in PMP beakers at ~ 70°C on a hotplate. As for the inverse aqua regia procedure, disposable 1 mL LPDE columns, quartz wool plugs, and Eichrom 1X8 100-200 mesh anion resin were used. After first cleaning the columns with 4 mL of 8N HNO_3 and equilibrating with 4 mL of 0.2N HCl, the sample precipitates were re-dissolved in 10 mL of MilliQ water and then loaded. The columns were washed with three portions of 4 mL of 1.0N HCl followed by 1 mL of 0.2N HNO_3, and 1.5 mL of 6N HNO_3. PMP beakers were again used to collect 3 mL of Re in 6N HNO_3. The Re solutions were then dried down in HEPA filtered air at ~ 60°C on a hotplate.

The dried Re precipitates were then further purified using single bead anion extraction. The precipitates were re-dissolved in 200 µL of 0.05N HNO_3 and each solution was placed into a 3 mL Savillex PFA Teflon vial with a DOWEX AGI-X8 < 20 mesh anion bead and left overnight on a rotator. Following absorption of the Re by the beads, these were then placed into new 3 mL Teflon vials with 1 mL of 6N HNO_3. These vials were rotated overnight to strip the Re from the beads. After discarding the beads to waste, the Re-HNO_3 solutions were subsequently dried down in HEPA filtered air on a hotplate at ~ 60°C.

Negative Thermal Ionization Mass Spectrometry

The dried Re samples were re-dissolved in 1 µL of 16N HNO_3 for at least 30 minutes before loading onto out-gassed (at a current of 1.6 A for 30 minutes) Ni filaments. The dried Os samples were dissolved in 0.5 µL of 9N HBr for at least one hour before loading onto Pt filaments. Before sample loading, the Pt filaments were first fluxed (using a procedure described by Morgan et al., 1995) and glowed for 30 minutes at a current of 3.0 A to minimize Os loading blank contributions. Both the Re and Os precipitates were loaded at a current of 1.0 A using a gas syringe and polyethylene tubing. To enhance the emission of negative ions, ~ 0.5 µL of $Ba(NO_3)_2$ was loaded onto the Re precipitates at a current of 1.0 A while ~ 0.25 µL of NaOH-$Ba(OH)_2$ was loaded onto the Os precipitates at a current of 0.5 A.

Analysis of the Re and Os isotopic compositions of the samples was carried out through NTIMS with a Micromass Sector 54 mass spectrometer equipped with nine Faraday collectors and a rear detector assembly comprising an off-axis electron multiplier (configured for both negative and positive ion detection) and an additional Faraday collector. Re and inverse aqua regia Os analyses were analyzed using the Faraday collectors in static mode while CrO_3-H_2SO_4 Os analyses were measured with the electron multiplier in single collector peak-hopping mode. The dominant molecular species measured in the negative ion beam are OsO_3^- and ReO_4^-. Isotopic oxide ratios were measured using mass numbers 234, 235, 236, 237, 238, and 240 for Os and 249 and 251 for Re. These oxide ratios were corrected for isobaric oxygen interferences to provide analyses of the metal isotopic ratios $^{185}Re/^{187}Re$, $^{186}Os/^{188}Os$, $^{187}Os/^{188}Os$, $^{189}Os/^{188}Os$, $^{190}Os/^{188}Os$, and $^{192}Os/^{188}Os$. Mass fractionation corrections (using $^{192}Os/^{188}Os = 3.08271$ and $^{185}Re/^{187}Re = 0.59738$) followed by corrections for blank and spike contributions were made to the Re and Os metal isotopic ratios. Total procedural blanks for samples dissolved with inverse aqua regia ranged from 1.7-4.5 pg and 1.7-3.1 pg for Re and Os, respectively, while the blank $^{187}Os/^{188}Os$ isotopic ratio ranged from 0.25 to 0.33. Re and Os blanks for the CrO_3-H_2SO_4 dissolution technique are 4.5 pg and 0.24 pg, respectively, with an average $^{187}Os/^{188}Os$ isotopic composition of 0.27 (Selby and Creaser, 2002). During the course of this study, an in-house Os laboratory standard (AB-2) was analyzed

repeatedly to provide a measure of mass spectrometer reproducibility. This standard yielded an $^{187}Os/^{188}Os$ isotopic ratio of 0.106833 ± 0.000100 (1σ, n=19) through Faraday collection analysis and 0.107060 ± 0.000429 (1σ, n=14) by electron multiplier analysis. To monitor reproducibility of $^{185}Re/^{187}Re$, an in-house Re standard solution was also analyzed and this yielded a value of 0.59843 ± 0.00060 (1σ, n=13). The measured sample $^{185}Re/^{187}Re$ isotopic ratios were corrected for the difference between the ratio of the in-house Re standard and the value of 0.59738 ± 0.00039 as determined by Gramlich et al. (1973).

RESULTS

Re and Os Concentrations and Isotope Variations

The Re and Os concentrations and isotope ratios for samples of the OFP slates obtained from both the inverse aqua regia and CrO_3-H_2SO_4 dissolution techniques are shown in table 1 while the results from inverse aqua regia analyses for samples of the UMG slates are given in table 2. The OFP samples have narrow ranges of Re (6.27-15.76 ppb) and Os (0.07-0.14 ppb) concentrations; an even more restricted range of Re (7.07-12.55 ppb) and Os (0.09-0.10 ppb) concentrations characterize the UMG slates. Both the Re and Os concentrations of the OFP samples as determined by CrO_3-H_2SO_4 dissolution are generally similar to the corresponding inverse aqua regia analyses. The Re and Os abundances of

Sample	Re (ppb)	Os (ppb)	$^{187}Re/^{188}Os$	$^{187}Os/^{188}Os$	$I_{Os(608)}$
BK-01-014A-WR	10.50	0.11	455.2	5.520 ± 0.009	0.89
BK-01-014A-WR-R	10.64	0.12	441.1	5.374 ± 0.002	0.88
BK-01-014A-OM	10.81	0.12	436.7	5.205 ± 0.013	0.76
BK-01-014A-OM-R	10.89	0.12	418.2	4.998 ± 0.004	0.74
BK-01-014B-WR	15.44	0.12	614.7	7.074 ± 0.003	0.82
BK-01-014B-WR-R	15.27	0.13	585.1	6.782 ± 0.003	0.82
BK-01-014B-WR-R2	15.33	0.12	596.3	6.906 ± 0.006	0.83
BK-01-014B-OM	15.76	0.13	595.1	6.718 ± 0.015	0.66
BK-01-014B-OM-R	15.50	0.14	525.4	5.954 ± 0.007	0.60
BK-01-015A-WR	6.27	0.10	287.8	3.679 ± 0.003	0.75
BK-01-015A-OM	6.44	0.11	277.1	3.471 ± 0.005	0.65
BK-01-015A-OM-R	6.39	0.12	263.3	3.299 ± 0.004	0.62
BK-01-015B-WR	12.17	0.12	491.0	5.747 ± 0.007	0.75
BK-01-015B-OM	12.59	0.13	464.4	5.352 ± 0.006	0.62
BK-01-015C-WR	8.38	0.12	331.2	4.127 ± 0.003	0.76
BK-01-015C-OM	8.58	0.13	319.1	3.859 ± 0.004	0.61
BK-01-015D-WR	7.15	0.07	476.8	5.774 ± 0.006	0.92
BK-01-015D-OM	7.31	0.09	380.1	4.475 ± 0.005	0.61

TABLE 1: Re and Os concentrations and isotope data for inverse aqua regia and CrO_3-H_2SO_4 analyses of the OFP slates. WR = whole-rock (inverse aqua regia analysis); OM = organic matter (CrO_3-H_2SO_4 analysis); R = replicate analysis; $I_{Os(608)}$ = initial $^{187}Os/^{188}Os$ isotope ratio at 608 Ma.

Sample	Re (ppb)	Os (ppb)	$^{187}Re/^{188}Os$	$^{187}Os/^{188}Os$	$I_{Os(590)}$
BK-01-009-WR	7.83	0.10	380.8	4.425 ± 0.004	0.66
BK-01-010-WR	7.07	0.09	362.7	4.248 ± 0.004	0.66
BK-01-011-WR	8.47	0.10	412.9	4.648 ± 0.003	0.57
BK-01-012-WR	7.43	0.09	401.3	4.815 ± 0.002	0.85
BK-01-013A-WR	12.55	0.10	615.6	6.265 ± 0.002	0.18
BK-01-013B-WR	11.51	0.10	531.4	5.571 ± 0.004	0.32

TABLE 2: Re and Os concentrations and isotope data for inverse aqua regia analyses of the UMG slates. WR = whole-rock (inverse aqua regia analysis); $I_{Os(590)}$ = initial $^{187}Os/^{188}Os$ isotope ratio at 608 Ma.

the carbonaceous slates from the OFP and UMG are significantly higher compared to the average Re (0.39ppb) and Os (0.05ppb) concentration of the continental crust (Esser and Turekian, 1993). The Re and Os concentrations and TOC contents of these samples are for the most part lower than for other ORMs previously dated with the Re-Os radioisotope system (Ravizza and Turekian, 1989; Cohen et al., 1999; Singh et al., 1999; Creaser et al., 2002).

The $^{187}Re/^{188}Os$ isotopic ratios of the OFP slates range from 263 to 615 while the $^{187}Os/^{188}Os$ isotopic ratios vary from 3.30 to 7.07. For each OFP sample, the $^{187}Re/^{188}Os$ and $^{187}Os/^{188}Os$ isotopic ratios obtained with inverse aqua regia are consistently higher than the corresponding analyses obtained by CrO_3-H_2SO_4 dissolution (although overlap does exist for some samples). The UMG slates display a more restricted range of $^{187}Re/^{188}Os$ (363 to 616) and $^{187}Os/^{188}Os$ (4.25 to 6.27) isotopic ratios. In both sample suites, these ratios are significantly more radiogenic than the corresponding average continental crust ratios ($^{187}Re/^{188}Os$ = ~ 48, $^{187}Os/^{188}Os$ = ~ 1.20-1.31; Esser and Turekian, 1993). Rapid changes (factors of ~ 2 to 3) in $^{187}Re/^{188}Os$ occurred over the ~ 50 cm stratigraphic sampling interval of both sample suites; such rapid variations were also observed over vertical scales of only 2 to 3 cm in the Jurassic ORMs from England (Cohen et al., 1999) and over <10 cm in the Exshaw Formation (Creaser et al., 2002).

Duplicate analyses (with the same dissolution technique) of the OFP samples show variable $^{187}Re/^{188}Os$ isotopic ratios that are positively correlated with changes in the corresponding $^{187}Os/^{188}Os$ isotopic ratios. This variation is probably caused by differences in Re and/or Os concentrations but this is not immediately clear because of the narrow concentration range in the data set. However, Creaser et al. (2002) observed that while the Re concentrations of duplicate analyses of Exshaw ORM samples were largely reproducible to better than ± 0.5%, they found that variations of up to ± 10% were present in the Os concentrations of some samples. These variations in Os concentration led to coupled variations in $^{187}Re/^{188}Os$ and $^{187}Os/^{188}Os$ and were suggested to result from the incomplete homogenization of the crushed sample powders. The contrast in reproducibility between Re and Os were interpreted as evidence that these elements may be present in different phases of ORMs. This is supported by the recent discovery of multiple Re complexes and/or bond types within the Exshaw ORMs (Selby and Creaser, 2002). Creaser et al. (2002) also found that duplicate analyses have similar initial $^{187}Os/^{188}Os$ isotopic ratios (I_{Os}) at the Exshaw Formation stratigraphic age of 364 Ma. Similarly, duplicate analyses of the OFP samples have approximately the same I_{Os} values at an age of 608 Ma (calculated below; see table 1). The coupled changes in the $^{187}Re/^{188}Os$ and $^{187}Os/^{188}Os$ isotopic ratios of duplicate analyses serve

only to introduce additional variation along a Re-Os isochron by providing further data points for regression.

Re-Os Age Determinations

The beta decay of ^{187}Re to ^{187}Os in ORMs can be expressed as a linear equation of the form $y = b + xm$:

$$\frac{^{187}Os}{^{188}Os} = I_{Os(t)} + \frac{^{187}Re}{^{188}Os}(e^{\lambda t} - 1)$$

where $^{187}Os/^{188}Os$ and $^{187}Re/^{188}Os$ are present-day isotopic ratios, $I_{Os(t)}$ represents the initial $^{187}Os/^{188}Os$ isotopic composition at time t (the depositional age of the sample or sample suite of interest in the case of a system closed to the gain or loss of Re and Os), and λ is the ^{187}Re decay constant. All Re-Os regressions were performed with the program *Isoplot* (Ludwig, 1998) which uses a ^{187}Re decay constant of 1.666×10^{-11} a^{-1} (Smoliar et al., 1996) and a 2σ confidence level. For the regressions, a ±1% uncertainty was assigned to all $^{187}Re/^{188}Os$ analyses while the measured $\pm 2\sigma_m$ of each sample $^{187}Os/^{188}Os$ isotopic ratio was used.

Regression of all nine inverse aqua regia analyses of the OFP slates yields a whole-rock errorchron with an age of 621 ± 28 Ma (MSWD = 6.9) and an I_{Os} value of 0.72 ± 0.23 (figure 3a). Much of the observed scatter can be attributed to BK-01-015D and two analyses of BK-01-014A; the data points from these two samples plot above the regression line. If these three analyses are excluded from the regression, a precise whole-rock age of 620.8 ± 8.1 Ma (MSWD = 0.9) and an I_{Os}

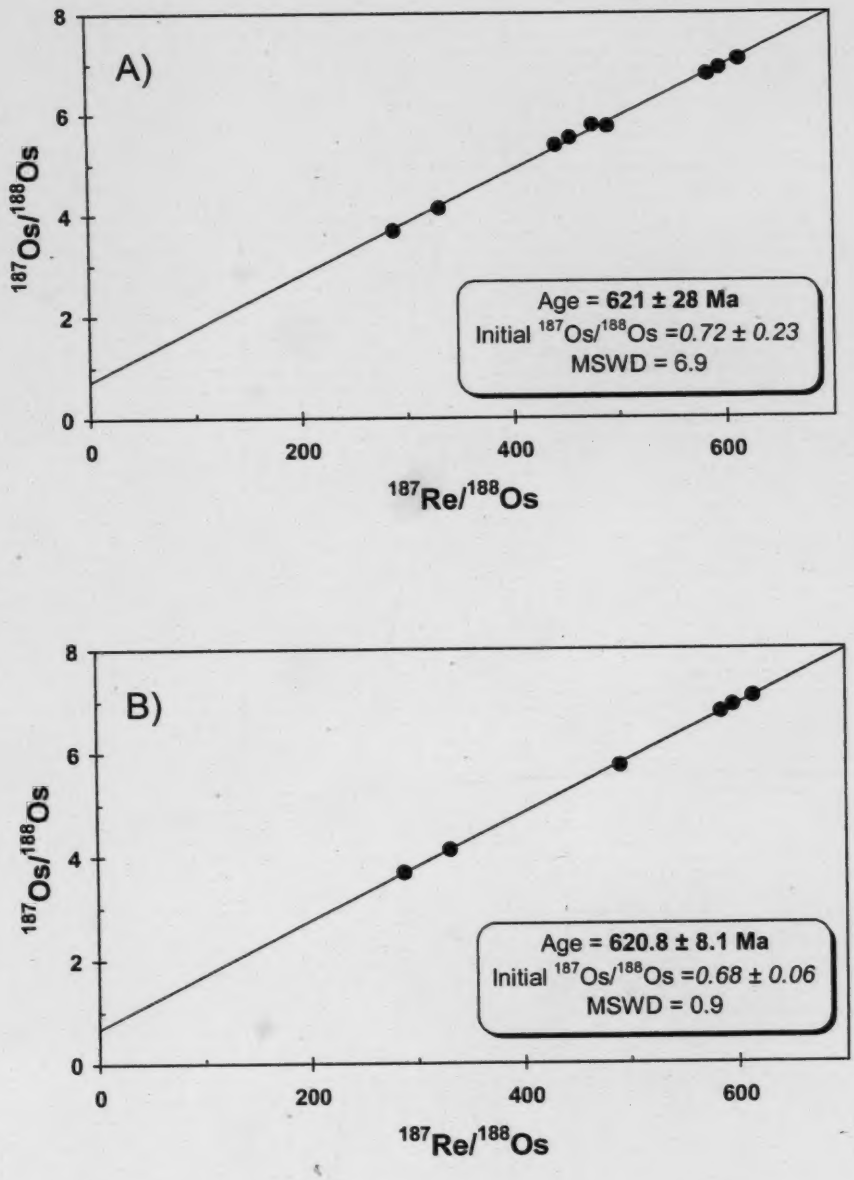

FIGURE 3: Re-Os isochron diagrams for OFP samples analyzed by conventional inverse aqua regia dissolution. A) All samples regressed. B) Regression with analyses of samples BK-01-014A and BK-01-015D excluded.

value of 0.68 ± 0.06 is obtained from the remaining six analyses of four samples (figure 3b). Similarly, if all nine OFP analyses obtained from the CrO_3-H_2SO_4 dissolution technique are regressed, an errorchron defining an age of 614 ± 53 Ma (MSWD = 27) and an I_{Os} value of 0.63 ± 0.37 is obtained (figure 4a). If two analyses of BK-01-014A are excluded (both plot above the regression line), regression of the remaining seven analyses of five samples yields a second precise age of 607.6 ± 8.3 Ma (MSWD = 1.4) and an I_{Os} value of 0.63 ± 0.05 (figure 4b).

The MSWD value (0.9) and calculated age uncertainty (1.3%) of the well-fitted inverse aqua region isochron represents a significant improvement in analytical precision over recent Re-Os studies of ORMs (MSWD > 1.6 and age uncertainties of 2-3%; Cohen et al., 1999; Singh et al., 1999; Schaefer and Burgess, 2001; Creaser et al., 2002). The precision of the 607.6 ± 8.3 Ma age obtained by CrO_3-H_2SO_4 digestion (MSWD = 1.4 and an age uncertainty of 1.4%) in this study is comparable to that of the best depositional age determinations of the Exshaw Formation (366.5 ± 3.5 Ma and 363.4 ± 5.6 Ma) obtained with this dissolution technique (MSWD values of 0.8 and 1.6; age uncertainties of 0.9% and 1.5%; Selby and Creaser, 2002).

To assess the influence of the non-hydrogenous component on the Re-Os systematics of the OFP slates, a direct comparison is made between the inverse aqua regia and CrO_3-H_2SO_4 dissolution techniques by regressing five analyses (one for each sample except for BK-01-014A

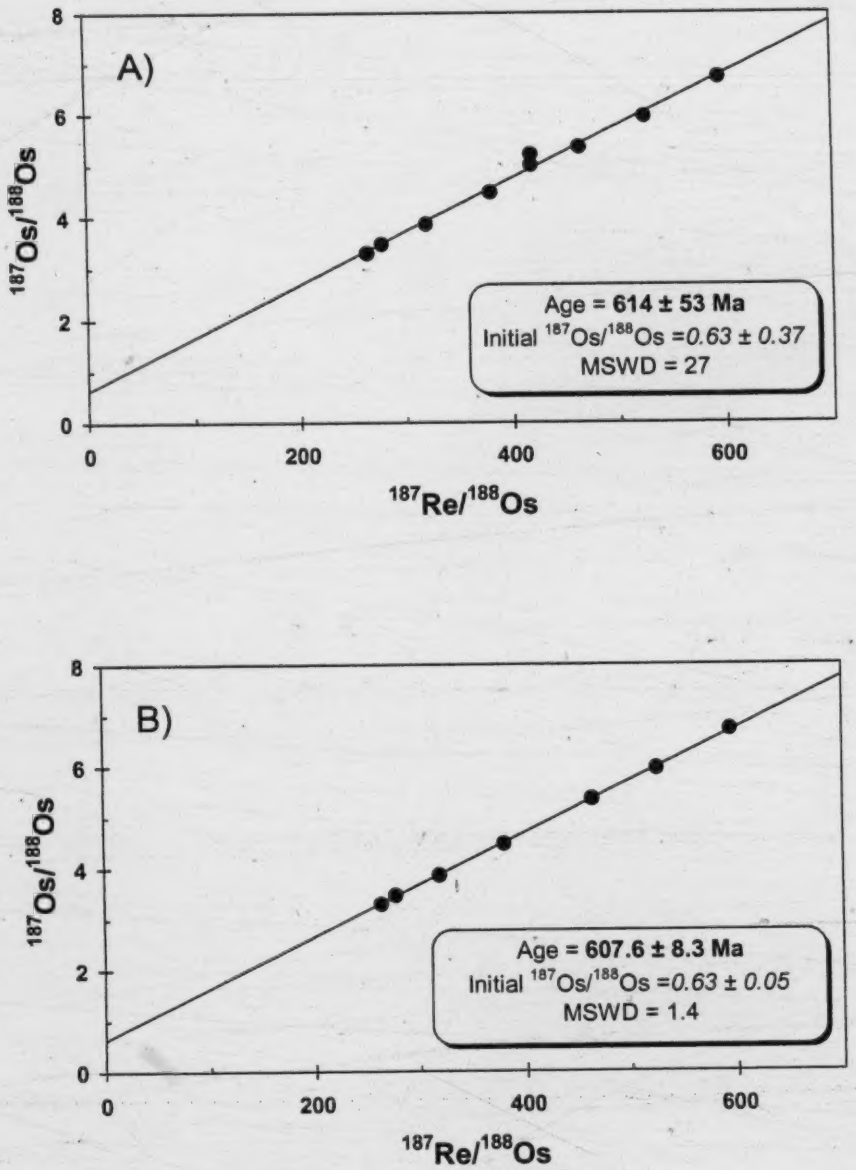

FIGURE 4: Re-Os isochron diagrams for OFP samples analyzed by CrO_3-H_2SO_4 dissolution. A) All samples regressed. B) Regression with sample BK-01-014A excluded.

as this sample plots above the regression line for both methods) that have the most similar $I_{Os(608\ Ma)}$ values (see table 1). While the inverse aqua regia data define an errorchron with an age of 623 ± 55 Ma (MSWD = 9.1; I_{Os} = 0.69 ± 0.42; figure 5a), regression of the CrO_3-H_2SO_4 analyses yields a very well-fitted isochron defining an age of 607 ± 11 Ma (MSWD = 0.2; I_{Os} = 0.62 ± 0.07; figure 5b). The implications of these results are discussed in a later section.

Inverse aqua regia analyses of six UMG samples define an errorchron with an age of 457 ± 84 Ma (MSWD = 52) and an I_{Os} value of 1.55 ± 0.65 (figure 6a). Sample BK-01-012 lies well above the regression line and is clearly responsible for most of the analytical scatter. Exclusion of this sample from the regression yields a well-fitted isochron defining an age of 471 ± 11 Ma (MSWD = 1.3) and an I_{Os} value of 1.40 ± 0.08 (figure 6b). This anomalously high I_{Os} value is more radiogenic than those obtained from other ORM horizons utilized in previous Re-Os dating studies (Ravizza and Turekian, 1989; Cohen et al., 1999; Singh et al., 1999; Creaser et al., 2002; Selby and Creaser, 2002).

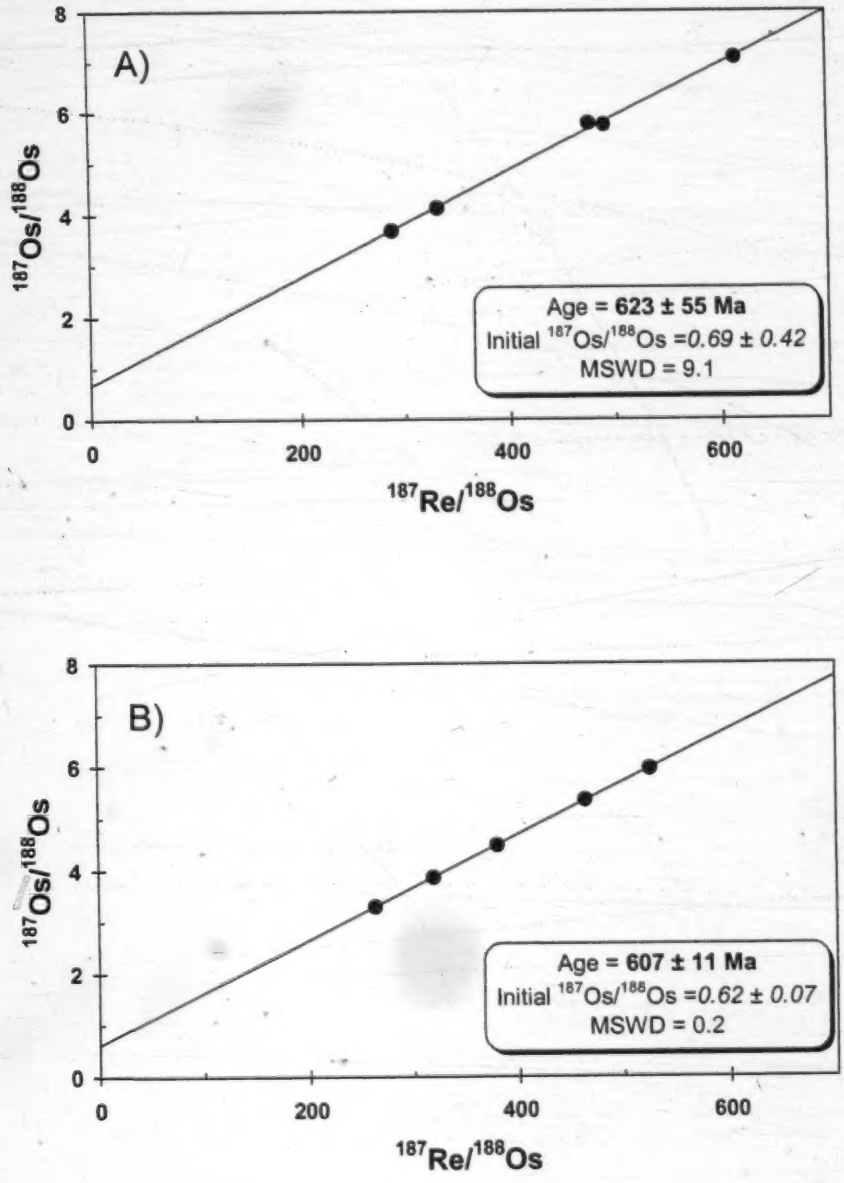

FIGURE 5: Comparative Re-Os isochron diagrams showing A) inverse aqua regia and B) CrO_3-H_2SO_4 regressions of one analysis of every sample except BK-01-014A. Analyses with the most similar initial $^{187}Os/^{188}Os$ isotope ratios at an age of 608 Ma (see table 1) were chosen for the regressions.

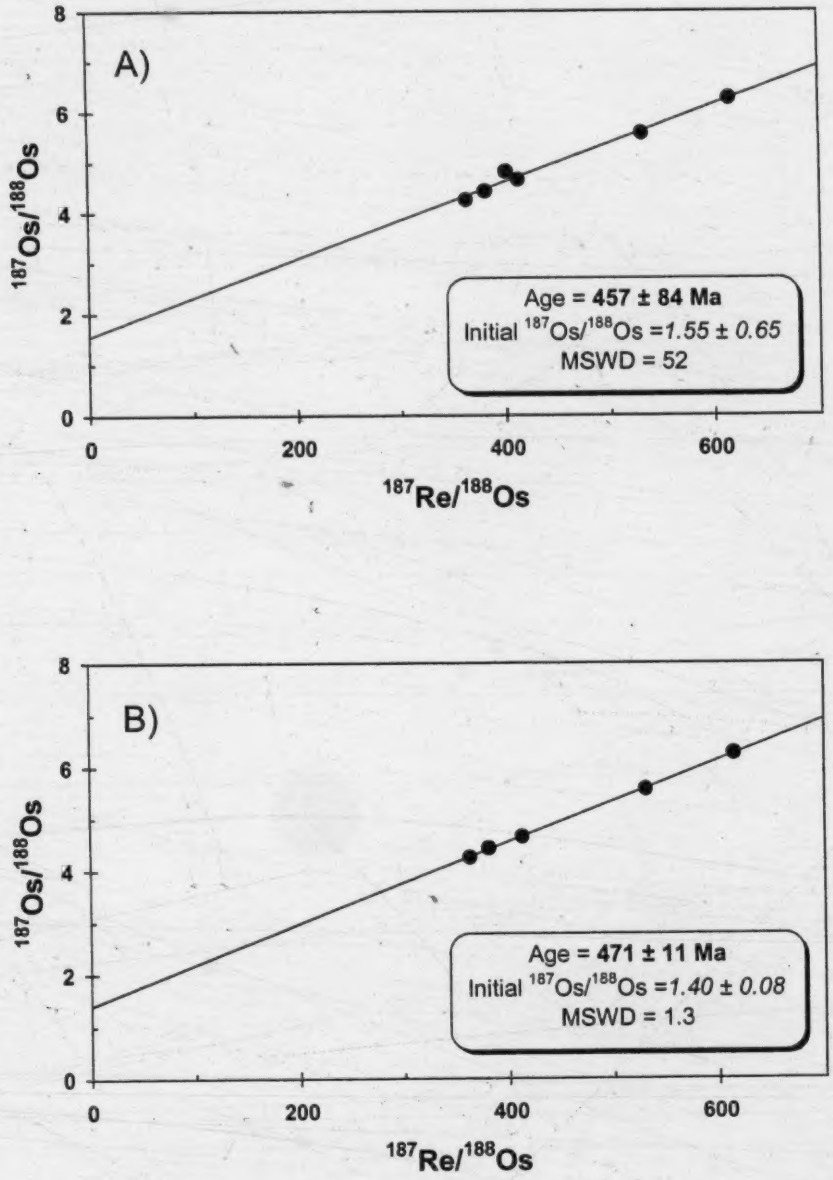

FIGURE 6: Re-Os isochron diagrams for UMG samples analyzed by conventional inverse aqua regia dissolution. A) All samples regressed. B) Regression with sample BK-01-012 excluded.

DISCUSSION

Re-Os Systematics of the OFP: Implications for Future Re-Os Dating of ORMs

To obtain precise and accurate depositional ages for ORMs with the ^{187}Re-^{187}Os radioisotope system, several assumptions must be met. ORMs must remain closed to Re and Os gain or loss during, or soon after, sediment deposition. The suite of ORM samples to be dated must all be the same age and have similar $I_{Os(t)}$ values (derived from the contemporaneous seawater). In addition, it is necessary to have a range in $^{187}Re/^{188}Os$ isotopic ratios that in turn generates a sufficient spread in $^{187}Os/^{188}Os$. The stratigraphic sampling interval (~ 50 cm in this study) must therefore be selected so as to obtain a good spread in $^{187}Re/^{188}Os$ isotopic ratios, yet avoiding the introduction of too much variation in $I_{Os(t)}$ values.

The precise ages of 620.8 ± 8.1 Ma and 607.6 ± 8.3 Ma obtained for the OFP slates with the inverse aqua regia and CrO_3-H_2SO_4 dissolution techniques fall within the range of existing absolute age constraints for the older Marinoan glacial interval (~ 620-600 Ma; Evans, 2000). These two ages are also consistent with the maximum ages reported for the Windermere Supergroup (762-728 Ma; Ross et al., 1995; Ross and Villeneuve, 1997) and with a U-Pb zircon age of 569.6 ± 5.3 Ma on volcanic rocks of the Hamill Group that

unconformably overlies the Windermere Supergroup (Colpron et al., 2002). The low MSWD values (0.9 and 1.4) of the two regressions suggest that most of the scatter along the isochrons can be attributed to analytical errors rather than geological perturbations. Thus, each of the two Re-Os ages individually appear (to a first approximation) to satisfy the basic assumptions outlined above for the Re-Os geochronometer. However, it will be demonstrated below that a detrital Re and Os component present in the OFP slates affected the calculated age and $I_{Os(t)}$ value obtained from the inverse aqua regia analyses.

The precise ages obtained in the present study have several implications for future Re-Os work on ORM horizons. It was only recently demonstrated that the Re-Os geochronometer was not disturbed during hydrocarbon maturation processes (temperatures up to 150°C; Creaser et al., 2002). The present study demonstrates for the first time that the Re-Os radioisotope system remained closed to the gain and/or loss of Re and Os during low-chlorite grade metamorphism. This is consistent with previous reports of closed-system behavior for the Re-Os geochronometer in other rock types exposed to greenschist-grade metamorphism (e.g., komatiite flows from the Abitibi Belt, Ontario, provided a Re-Os crystallization age of 2726 ± 93 Ma; Walker et al., 1988). Secondly, it is possible to obtain precise Re-Os ages on ORMs from samples collected from outcrop rather than drillcore, provided the necessary precautions are taken to ensure the analyzed material is fresh

(i.e., collecting large, thick samples and removing the weathered outer surfaces). These steps ensure that any loss of Re, Os, and organic carbon, and thus disturbance of the Re-Os system, from weathering processes is minimized (e.g., Peucker-Ehrenbrink and Hannigan, 2000; Jaffe et al., 2002; Pierson-Wickmann et al., 2002). Although drill core samples of ORMs would remove the issue of surface weathering from consideration altogether (Creaser et al., 2002), it is not a mandatory sample collection protocol necessary for obtaining Re-Os depositional ages from ORMs. Finally, although it is always preferable to collect ORM samples with high TOC contents (i.e., > 5%; Cohen et al., 1999; Creaser et al., 2002) in order to obtain high Re and Os concentrations and maximize the hydrogenous fraction of Re and Os, it is not a prerequisite for obtaining precise depositional ages as the OFP slates analyzed in the present study contain < 0.5% TOC.

By utilizing the inverse aqua regia and CrO_3-H_2SO_4 dissolution techniques, the proportion of non-hydrogenous Re and Os in the OFP slates can be evaluated. The inverse aqua regia method provides a "whole-rock" Re-Os analysis of an ORM sample because it includes Re and Os derived from hydrogenous and non-hydrogeneous (detrital and meteoritic particulate) sources (Selby and Creaser, 2002). If the proportion of detrital or extraterrestrial Re and Os is significant (i.e., several percent or more of the hydrogenous Re and Os budget), this may have an impact on the calculated depositional age and $I_{Os(t)}$ value of an

ORM sample suite. For example, Creaser et al. (2002) presented evidence for an unradiogenic detrital and/or extraterrestrial Os component in ORMs from the Exshaw Formation. If approximately 0.01 ppb of Os within ORMs is derived from detrital sources (i.e., 20% of the average continental crust abundance of 0.05 ppb; Esser and Turekian, 1993; Cohen et al., 1999), the detrital Os budget would make up 7.1-14.3% of the OFP slates. If the non-hydrogenous component is dominated by a detrital source that is more radiogenic than the hydrogenous Os component, the calculated depositional age of an ORM sample suite will be erroneously older and the $I_{Os(t)}$ value higher. On the other hand, a less radiogenic detrital and/or meteoritic particulate component will have the opposite effect. Such contamination would likely become more significant in ORMs containing low TOC (< 1%) since the hydrogenous Re and Os budget would be smaller.

The CrO_3-H_2SO_4 dissolution technique excludes any detrital Re and Os by selectively dissolving the organic matter (Selby and Creaser, 2002) and thus provides an "organic matter" age. This procedure would still include any Re and Os derived from undissolved extraterrestrial material (e.g., Re- and Os-rich phases such as hydrocarbons and sulfides). However, the total Re and Os extraterrestrial component (both the particulate and dissolved forms) is expected to be small (0.2-0.4%) for the OFP slates if the meteorite fluxes at ~ 608 Ma (currently unknown) are similar to that of the Cenozoic (e.g., a meteorite flux of ~ 3.7×10^4 T/a, a

chondritic meteorite Os concentration of 486 ppb, and an ORM accumulation rate of 50 m/Ma yields a meteoritic Os contribution of ~ 0.28 x 10^{-12} g Os/g ORM; Cohen et al., 1999). However, if the ~ 608 Ma meteorite fluxes were higher or the ORM sedimentation rate anomalously low, then the extraterrestrial Re and Os budget in the OFP slates may be larger. Nevertheless, the CrO_3-H_2SO_4 dissolution technique should provide a more accurate Re-Os depositional age and $I_{Os(t)}$ determination for an ORM sample suite; the latter reflects the Os isotopic composition of the contemporaneous seawater at the time of sediment deposition (Selby and Creaser, 2002).

A comparison of the Re-Os data set obtained by the two dissolution techniques reveals the presence of a radiogenic detrital Re and Os component in the OFP slates. This is reflected by consistently higher $^{187}Re/^{188}Os$ and $^{187}Os/^{188}Os$ isotopic ratios and $I_{Os(608\ Ma)}$ values of inverse aqua regia analyses of each OFP sample compared to the corresponding CrO_3-H_2SO_4 analyses (see table 1 and figure 7). In addition, regression of five CrO_3-H_2SO_4 analyses (one from each sample except BK-01-014A) with the most similar $I_{Os(608\ Ma)}$ values produced a better isochron (defining an age of 607 ± 11 Ma with an MSWD of 0.2) than that of the corresponding inverse aqua regia analyses (623 ± 55 Ma; MSWD = 9.1) (see figure 6). Much of the difference in the precision of the two methods is attributable to sample BK-01-015D. While this sample lies on the CrO_3-H_2SO_4 regression line, it plots above the inverse aqua regia

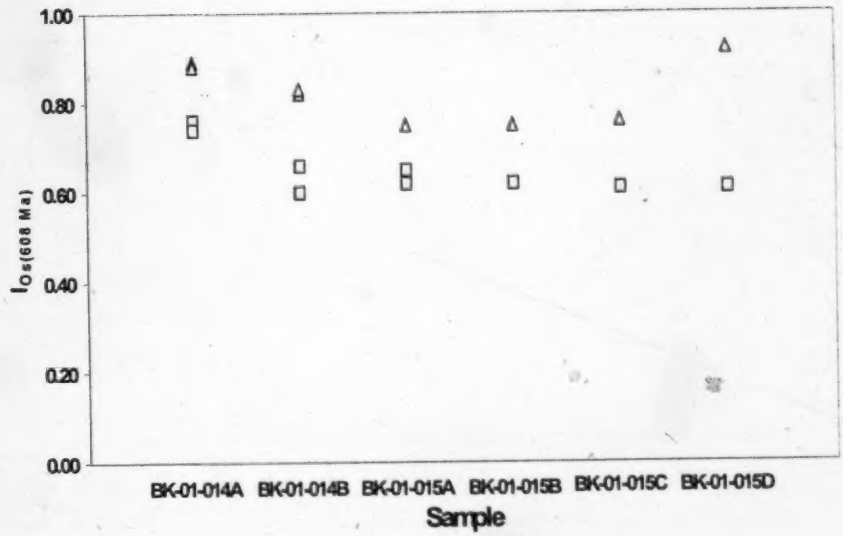

FIGURE 7: Initial $^{187}Os/^{188}Os$ isotopic ratios (I_{Os}) for each OFP sample at 608 Ma. Triangles = inverse aqua regia analyses. Squares = CrO_3-H_2SO_4 analyses.

isochron. However, the precise inverse aqua regia age (620.8 ± 8.1 Ma) and I_{Os} value (0.68 ± 0.06) obtained by excluding this sample is still noticeably higher (although equivalent within the assigned 2σ analytical uncertainties) than the precise age (607.6 ± 8.3 Ma) and I_{Os} value (0.63 ± 0.05) obtained from the CrO_3-H_2SO_4 dissolution technique. The evidence of radiogenic detrital Re and Os contamination in the low-TOC OFP slates outlined here provides further support to the CrO_3-H_2SO_4 dissolution technique of Selby and Creaser (2002) as a superior method to inverse aqua regia for determining precise and accurate depositional ages and $I_{Os(t)}$ values for ORMs. Thus, I consider 607.6 ± 8.3 Ma to be the best depositional age determination of the OFP and 0.63 ± 0.05 to be the best estimate of the local seawater $^{187}Os/^{188}Os$ isotopic composition at that time.

Implications for the Neoproterozoic Glaciations

The OFP has previously been interpreted as the product of a post-glacial eustatic sea-level rise that followed the meltback of the second Windermere ice age (Ross, 1991a; Ross et al., 1995). As described in a previous section, lithological similarities and carbon isotopic data together suggest the OFP to be stratigraphically comparable to cap carbonates overlying the diamictites of the Mount Vreeland Formation in northeastern British Columbia and the Ice Brook Formation in the Mackenzie Mountains, N.W.T. The Re-Os depositional age of 607.6 ±

8.3 Ma obtained for the OFP carbonaceous interval thus provides a minimum age constraint for these glacial intervals. The second Windermere glaciation likely falls within the ~ 620-600 Ma time interval assigned to the older Marinoan/Varanger ice age (based largely on U-Pb dating of several Neoproterozoic glaciogenic deposits worldwide; Evans, 2000; table 3). The Mount Vreeland and Ice Brook diamictites are also similar in age to the Nantuo glacial deposits of southern China which have minimum age constraints of 584 ± 26 Ma and 599.3 ± 4.2 Ma (obtained from the Lu-Hf and Pb-Pb dating, respectively, of phosphorites from the disconformably overlying Doushantuo Formation; Barfod et al., 2002).

In contrast, other Neoproterozoic glacial deposits from northeastern North America appear to represent a younger Marinoan glacial epoch. The age of the glaciogenic Gaskiers Formation on the Avalon Peninsula of Newfoundland is constrained between 565 ± 3 Ma and 606 +3.7/-2.9 Ma by U-Pb dating of ash beds (Krogh et al., 1988; Benus, 1988). A maximum U-Pb age of 596 ± 2 Ma for the Squantum tillite in the Boston Basin, Massachusetts, is provided by a welded tuff clast within the tillite (Thompson and Bowring, 2000). Similar ages were also found in detrital zircons from underlying sandstones. A minimum age of ~ 570 Ma is inferred for this glacial deposit based on the youngest U-Pb zircon dates from an ash bed in the overlying Cambridge Argillite (Thompson and Bowring, 2000). However, further radiometric dating

Glacial Interval	Older Marinoan (620 – 600 Ma)		Younger Marinoan (580 – 570 Ma)	
	Glacial Deposit	Age	Glacial Deposit	Age
Minimum Age Constraints	Nantuo (China)[1]	584 ± 26 Ma (Lu-Hf) 599.3 ± 4.2 Ma (Pb-Pb)	Gaskiers (Canada)[4]	565 ± 3 Ma (U-Pb)
	Mount Vreeland and Ice Brook (Canada)[2]	607.6 ± 8.3 Ma (Re-Os)	Squantum (Northeast U.S.)[5]	570 Ma (U-Pb)
	Various glacial deposits from the Congo-Sao Francisco and Western Africa[3]	600 Ma (U-Pb) 620 Ma (U-Pb)		
Maximum Age Constraints	None		Squantum (Northeast U.S.)[5]	596 ± 2 Ma (U-Pb)
			Loch na Cille (Scotland)[6]	601 ± 4 Ma (U-Pb)
			Gaskiers (Canada)[7]	606 +3.7/-2.9 Ma (U-Pb)

TABLE 3: Summary of known geochronological age constraints on Marinoan glacial deposits. 1 – Barfod et al. (2002); 2 – Present study; 3 – Evans (2000); 4 – Benus (1988); 5 – Thompson and Bowring (2000); 6 – Dempster et al. (2002); 7 – Krogh et al. (1988).

studies are needed on other continents to demonstrate the areal extent of the younger Marinoan/Varanger glaciation (Evans, 2000). As a first step in this direction, a U-Pb zircon age of 601 ± 4 Ma was recently reported for the Tayvallich Volcanic Formation of the Dalradian Supergroup in the Scottish Highlands; this age provided a maximum age constraint on the timing of the Loch na Cille glaciation (Dempster et al., 2002). The Marinoan glacial interval in the Amadeus Basin of Australia has been assigned a maximum age constraint of 592 ± 14 Ma (preliminary Re-Os age on ORMs from the Aralka Formation that underlies the diamictites; Schaefer and Burgess, 2001) that is intermediate between the two recognized Marinoan glacial intervals. However, this study employed an inverse aqua regia procedure modified from that of the present study (B. F. Schaefer, personal communication, 2002). Because the Aralka age may therefore be influenced by a detrital Re and Os component, it is considered suspect and should be treated with caution.

The successful application of the Re-Os radioisotope system to the OFP slates suggests that this geochronometer can be applied to other weakly- to non-metamorphosed ORMs that are temporally and spatially related to Neoproterozoic glaciogenic deposits. As in the case of the OFP, the post-glacial eustatic sea-level rise that follows the meltback stage of a Neoproterozoic ice age can lead to the deposition of areally extensive ORMs that are stratigraphically comparable to and/or overlie cap carbonates of the Neoproterozoic diamictites. As an example, within

the Adelaide Geosyncline of Australia, the Tindelpina Shale Member of the basal Tapley Hill Formation overlies the glaciogenic Wilyerpa Formation (McKirdy et al., 2001). ORMs may also be found underlying Neoproterozoic glaciogenic deposits (e.g., the previously described Aralka Formation; Schaefer and Burgess, 2001) if an anoxic paleogeographic environment (e.g., within a deep borderland basin or on a passive margin continental slope; Arthur and Sageman, 1994) existed prior to the onset of glacial conditions. However, it is likely that ORMs formed in response to an eustatic post-glacial sea-level rise are a more common occurrence and these ORMs would thus represent a better target for Neoproterozoic Re-Os dating studies.

The ability to provide absolute age constraints on Neoproterozoic glacial deposits through the Re-Os dating of ORMs is important because there is a paucity of suitable igneous rocks that are associated with the diamictites and are amenable to radiometric dating methods. Currently, the absolute age constraints on most individual Neoproterozoic glacial intervals are weak. Many of these diamictites were previously assigned age constraints using the ^{87}Rb-^{87}Sr system (e.g., on associated shales) but subsequent studies have demonstrated that this system is unreliable for determining depositional ages (i.e., because of detrital effects; Evans, 2000). Current age constraints (largely provided by the U-Pb dating of zircons from ash beds) are not sufficient to determine precisely the number of Neoproterozoic ice ages or their timing, duration, and extent.

Widespread application of the Re-Os geochronometer to Neoproterozoic ORMs should provide improved age constraints on many of the previously undated or poorly dated Neoproterozoic glaciogenic deposits. In the case of ORMs such as the OFP that are stratigraphically comparable to cap carbonates, Re-Os depositional ages will allow the negative $\delta^{13}C$ isotopic excursions of the carbonates to be directly dated. Improved age constraints on Neoproterozoic glacial intervals will facilitate their correlation worldwide and allow a more accurate assessment of the Snowball Earth theory and its prediction of global, synchronous glaciations.

In previous years, the lack of both precise geochronological constraints and a diverse biostratigraphy in the Neoproterozoic rock record led researchers to use carbon (and also strontium and sulphur) isotopic excursions as a means of correlating the glacial deposits (e.g., Walter et al., 2000) and to provide information on the number of Neoproterozoic ice ages and their time duration. Unfortunately, controversy has resulted from this method. As an example, on the basis of carbon and strontium isotope correlations between the Canadian, Spitsbergen, Namibian, and Australian Neoproterozoic rock records and considering the known occurrences of Ediacaran fossils in each region, Kaufman et al. (1997) suggested there were at least four discrete Neoproterozoic ice ages. However, Kennedy et al. (1998) argued, using a cladistic analysis of several lithological and geochemical indicators on

twelve Neoproterozoic glaciogenic deposits, that there were only two. Because a unique carbon isotope signature apparently does not characterize each individual Neoproterozoic glaciation, the number of ice ages is unknown.

In addition, the origin of the negative $\delta^{13}C$ isotopic excursions within the cap carbonates is currently disputed. The Snowball Earth theory suggests the excursions may have lasted throughout the glaciation as a result of a nearly complete decline in biological productivity (this leads to mantle $\delta^{13}C_{carb}$ values in syn-glacial carbonates) with the negative $\delta^{13}C_{carb}$ values in the cap carbonates resulting from large alkalinity fluxes during post-glacial weathering processes (Hoffman et al., 1998a, b; Hoffman and Schrag, 2000, 2002). On the other hand, the excursions may represent a purely post-glacial phenomenon related to the precipitation of cap carbonates during the destabilization of gas hydrates in terrestrial permafrost on flooded continental shelves and basins (Kennedy et al., 2001a). A gas hydrate origin has been supported by the discovery of positive $\delta^{13}C_{carb}$ values from in-situ carbonates within several different Neoproterozoic glaciogenic deposits (Kennedy et al., 2001b). However, Hoffman and Schrag (2002) point out that tube structures, which could have served as methane gas migration pathways within the cap carbonates (Kennedy et al., 2001a), do not extend down into the underlying glacial deposits. Hoffman et al. (1998a, b) determined a minimum time span of at least ~ 9 Ma for the duration of the negative

$\delta^{13}C$ isotopic excursion that brackets the Ghaub glacial interval. This calculation was based on maximum thermal subsidence rates for the Otavi carbonate platform of Namibia. On the other hand, Kennedy et al. (1998) did not find evidence of any negative $\delta^{13}C$ isotopic excursion beneath the Ghaub glacial interval despite analyzing carbonate samples from the same measured section as Hoffman et al. It therefore seems clear that chemostratigraphic studies alone cannot provide unambiguous information on the duration and extent of the Neoproterozoic ice ages. Only precise absolute age determinations (employing the Re-Os, U-Pb, and, more rarely, other radioisotope systems where applicable) of suitable geological materials associated with the Neoproterozoic glacial deposits can truly provide reliable and accurate constraints on the number of Neoproterozoic ice ages and their timing, duration, and extent.

$^{187}Os/^{188}Os$ Isotopic Composition of ~ 608 Ma Neoproterozoic Seawater

The $I_{Os(608\ Ma)}$ value of 0.63 ± 0.05 calculated from the regression of the CrO_3-H_2SO_4 analyses for the OFP slates best reflects the contemporaneous Os isotopic composition of the local ~ 608 Ma seawater and also that of the open ocean if the two were thoroughly mixed. This was likely the case since the Windermere basin was situated on a west-facing passive continental margin (Ross, 1991b; Ross et al., 1995) or within a 2500 km long intracontinental rift connected to a northern ocean basin (Colpron et al., 2002). The $^{187}Os/^{188}Os$ isotopic composition of

~ 0.63 for ~ 608 Ma seawater is significantly less radiogenic than that of present-day seawater (~ 1.04-1.07; Sharma et al., 1997; Levasseur et al., 1998; Woodhouse et al., 1999). The cause for the relatively unradiogenic Neoproterozoic seawater $^{187}Os/^{188}Os$ signature can be understood by first considering the different sources of Os to the present-day ocean and their $^{187}Os/^{188}Os$ isotopic compositions, both of which are now reasonably well understood.

Dissolved (hydrogenous) osmium in seawater is supplied by continental, mantle, and extraterrestrial sources (figure 8; Palmer et al., 1988; Sharma et al., 1997). The continental Os component consists largely of radiogenic Os derived from continental weathering and transported to the oceans via rivers. Sources of this component include radiogenic contributions from black shales (Pierson-Wickmann et al., 2000) and Precambrian shields (Peucker-Ehrenbrink and Ravizza, 1996; Peucker-Ehrenbrink and Blum, 1998), but also unradiogenic Os from ophiolites (Pegram et al., 1994) and arc-related crust (Martin et al., 2000). An unradiogenic upper mantle Os component is provided by the low temperature hydrothermal alteration of off-axial juvenile mid-ocean ridge basalts (Sharma et al., 2000) and back-arc basalts. Hydrothermal contributions would also be expected from hot spots. Another unradiogenic source of Os is provided by the dissolution of cosmic dust in seawater (Palmer et al., 1988; Sharma et al., 1997). While ^{187}Os can also be added to seawater through the beta decay of ^{187}Re, this contribution is

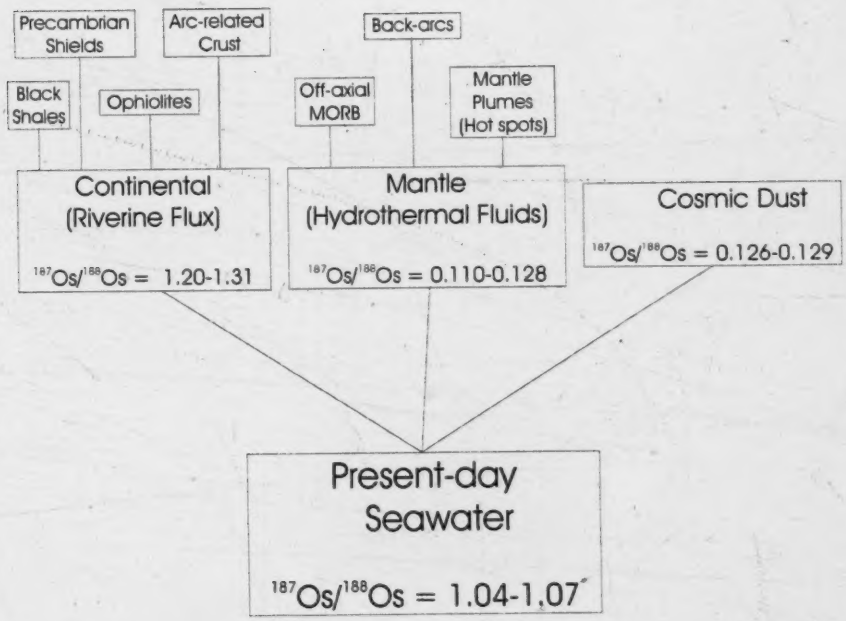

FIGURE 8: Compositions of the known Os sources to present-day seawater. See text for discussion and sources of data.

several orders of magnitude lower than that of the other sources of Os to seawater and is thus not considered (i.e., Singh et al., 1999). The average $^{187}Os/^{188}Os$ isotopic composition of the continental crust is ~ 1.20-1.31 (Esser and Turekian, 1993) while upper mantle Os (derived from hydrothermal fluids) ranges from 0.110 (depleted) to 0.128 (primitive upper mantle) (Sharma et al., 2000; Walker et al., 2002). Chondritic meteorites have values of 0.126 to 0.129 (Meisel et al., 1996) that are comparable to the primitive upper mantle, but the hot spot $^{187}Os/^{188}Os$ isotopic signature is often slightly more radiogenic (~ 0.13-0.16; Hauri and Hart, 1993; Reisberg et al., 1993).

The more unradiogenic $^{187}Os/^{188}Os$ isotopic ratio of ~ 0.63 for Neoproterozoic seawater compared to the values of ~ 1.04-1.07 for present-day seawater reflects increased hydrothermal activity at rift margins, hot spots, and backarcs, more intensive weathering of arc-related crust and ophiolites, larger frequencies of bolide impacts, and/or decreased continental weathering rates at ~ 608 Ma. Although a method to resolve the relative contributions of mantle Os from dissolved extraterrestrial inputs is not available, increased hydrothermal activity is expected to be an important source of unradiogenic seawater Os as rifting along the western-southwestern margin of Laurentia culminated in fragmentation from Rodinia during the Marinoan glaciation (Prave, 1999; Colpron et al., 2002). An $^{187}Os/^{188}Os$ isotopic ratio of ~ 0.63 suggests at least a moderate continental Os input to ~ 608 Ma seawater. However,

unradiogenic seawater $^{87}Sr/^{86}Sr$ isotopic ratios (e.g., 0.7071; correction for diagenetic effects suggests even lower values such as 0.7053) were obtained from the correlative Teepee Dolomite in the Mackenzie Mountains (Narbonne et al., 1994; Kaufman et al., 1997; James et al., 2001). This suggests that significant runoff of glacial debris into the oceans was either not yet important or did not affect the $^{87}Sr/^{86}Sr$ isotopic composition of seawater (James et al., 2001). The latter possibility suggests that the riverine Os flux to ~ 608 Ma seawater may have been more unradiogenic compared to the present-day. If the observed unradiogenic $^{87}Sr/^{86}Sr$ isotopic ratios for the Teepee Dolomite are in fact pre-dating significant fluvioglacial runoff, the contrasts between the Sr and Os isotopic records reflect the seawater residence time of Os (< 12 ka to 54 ka; Sharma and Wasserburg, 1997; Sharma et al., 1997, 2000; Oxburgh, 1998, 2001; Levasseur et al., 1999, 2000) being two orders of magnitude shorter than that of strontium.

One sample (BK-01-014A) has significantly higher $I_{Os(608\ Ma)}$ values (0.74 and 0.76) from CrO_3-H_2SO_4 analyses compared to the other samples and was also collected at the highest stratigraphic level of the sampled OFP carbonaceous interval. This suggests that the seawater $^{187}Os/^{188}Os$ isotopic composition evolved over time to higher values during deposition of the OFP carbonaceous slates although the time duration over which this occurred cannot be determined because the sediment accumulation rate for the carbonaceous interval is not known.

Re-Os Isotope Systematics and Metamorphism

Before the Re-Os radioisotope system can be applied routinely to ORMs of any age, the limitations of this geochronometer must be fully understood. This includes any post-depositional processes that could cause open-system Re-Os behavior such that depositional age determinations are not possible. The detrimental effects of weathering processes on the Re-Os systematics in ORMs are now reasonably well understood (Peucker-Ehrenbrink and Hannigan, 2000; Jaffe et al., 2002; Pierson-Wickmann et al., 2002). However, before the present study was undertaken, the response of the Re-Os radioisotope system in ORMs to prograde metamorphism was not known. This topic is especially important for Neoproterozoic and other Precambrian ORMs since these ancient clastic sedimentary rocks are often more metamorphosed than their Phanerozoic counterparts.

It was demonstrated in a previous section that Re and Os remained a closed system within the OFP slates during low chlorite-grade metamorphism. The study of the UMG slates examines the effect of middle-chlorite grade metamorphism on the Re-Os systematics of ORMs. Five of the inverse aqua regia analyses from the UMG slates define a well-fitted isochron corresponding to an apparent age of 471 ± 11 Ma (MSWD = 1.3) and an I_{Os} value of 1.40 ± 0.08. However, this age is not in agreement with existing age constraints that bracket the UMG between a maximum age of 607.6 ± 8.3 Ma (depositional age of the OFP

carbonaceous interval determined in the present study) and a minimum age of 569.6 ± 5.3 Ma (Hamill Group volcanic rocks; Colpron et al., 2002). The I_{Os} value from the UMG regression is also significantly more radiogenic than that calculated for ORMs in previous Re-Os dating studies (Ravizza and Turekian, 1989; Cohen et al., 1999; Singh et al., 1999; Creaser et al., 2002; Selby and Creaser, 2002) or determined for present-day seawater ($^{187}Os/^{188}Os$ = 1.04-1.07; Sharma et al., 1997; Levasseur et al., 1998; Woodhouse et al., 1999). These observations suggest that some process has disturbed the Re-Os system in the UMG slates such that a meaningless average (~ 471 Ma) of the true depositional (~ 590 Ma) and metamorphic (~ 100-45 Ma) ages was obtained.

The UMG slates contain unaltered, fresh pyrite nodules similar to that of the OFP and thus any major losses of Re and Os by weathering mechanisms is not expected. Diagenetic alteration of the Re-Os systematics is also unlikely because previous studies have shown that diagenetic pyrite nodules (and hence the pore fluids) contain very low levels of Re and Os compared to the host ORMs (Cohen et al., 1999; Pierson-Wickmann et al., 2000). Although the CrO_3-H_2SO_4 dissolution technique was not applied to the UMG slates, detrital contamination is not expected to account for the nearly 100 Ma difference between the expected age (~ 590 Ma) and the observed inverse aqua regia age (~ 471 Ma). This is a reasonable assumption because the lower-TOC

OFP slates yielded two precise ages with both dissolution techniques that were still equivalent within the assigned 2σ analytical uncertainties.

Because Re and Os are associated with organic matter (Ravizza et al., 1991; Ravizza and Turekian, 1992; Ravizza and Esser, 1993; Cohen et al., 1999; Martin et al., 2000; Peucker-Ehrenbrink and Hannigan, 2000; Pierson-Wickmann et al., 2000, 2002; Jaffe et al., 2002), disturbance of the Re-Os system during thermal alteration of organic matter is expected. With increasing temperature, carbonaceous matter undergoes a complex series of transformations that ultimately result in the formation of crystalline graphite (termed the graphitization process; Hoefs and Frey, 1976). This process involves the preferential thermal cracking of ^{12}C-^{12}C bonds and the release of ^{12}C-rich fluids (as CH_4 or CO_2) in hydrocarbon maturation reactions (Stahl, 1974). As a result, the organic matter residue becomes progressively enriched in ^{13}C. This process can continue until fully ordered graphite forms at 500°C (Landis, 1971; Hoefs and Frey, 1976). If any carbonate minerals are present within ORMs, exchange of carbon between the organic and carbonate fractions will also occur. Such carbon isotope exchange can begin at temperatures as low as 300°C; however, the exchange is kinetically slow and limited by the organic fraction; the two carbon reservoirs do not reach equilibrium until temperatures higher than 650°C are reached (Valley and O'Neil, 1981; Chacko et al., 1991).

The overall effect of the hydrocarbon maturation and carbon isotope exchange reactions is an increase in $\delta^{13}C_{org}$ and a decrease in $\delta^{13}C_{carb}$ with a resulting decrease in $\Delta^{13}C_{carb\text{-}org}$ of ORMs as higher metamorphic temperatures are reached. Increases in $\delta^{13}C_{org}$ with progressively higher grades of metamorphism have been observed previously in ORMs (e.g., McKirdy et al., 1975; Hoefs and Frey, 1976). Significantly, the data of Hoefs and Frey (1976) show that the $\delta^{13}C$ values of organic carbon in the Liassic black shale series of the Swiss Alps do not become systematically higher with increasing metamorphic grade until ~ 350°C (figure 9). The most significant increases in $\delta^{13}C_{org}$ for the Liassic black shales occur during upper chlorite-grade metamorphism (~ 400°C). At 350°C, middle-chlorite grade slates have $\delta^{13}C_{org}$ values of -23‰ to -22‰ compared to a value of -25‰ for the unmetamorphosed protoliths (Hoefs and Frey, 1976). It therefore seems plausible that the $\delta^{13}C_{org}$ values of the unmetamorphosed UMG shales may also have been increased by 2-3‰ to the observed values of -29‰ to -25‰ during middle chlorite-grade metamorphism. These observations suggest that disturbance of the Re-Os system in the UMG slates is likely related to the thermally-induced changes in organic carbon isotopes occurring at ~ 350°C.

Could either hydrocarbon maturation or carbon isotope exchange reactions between carbonate and organic matter be directly responsible for disturbing the Re-Os systematics of the UMG slates? The former may

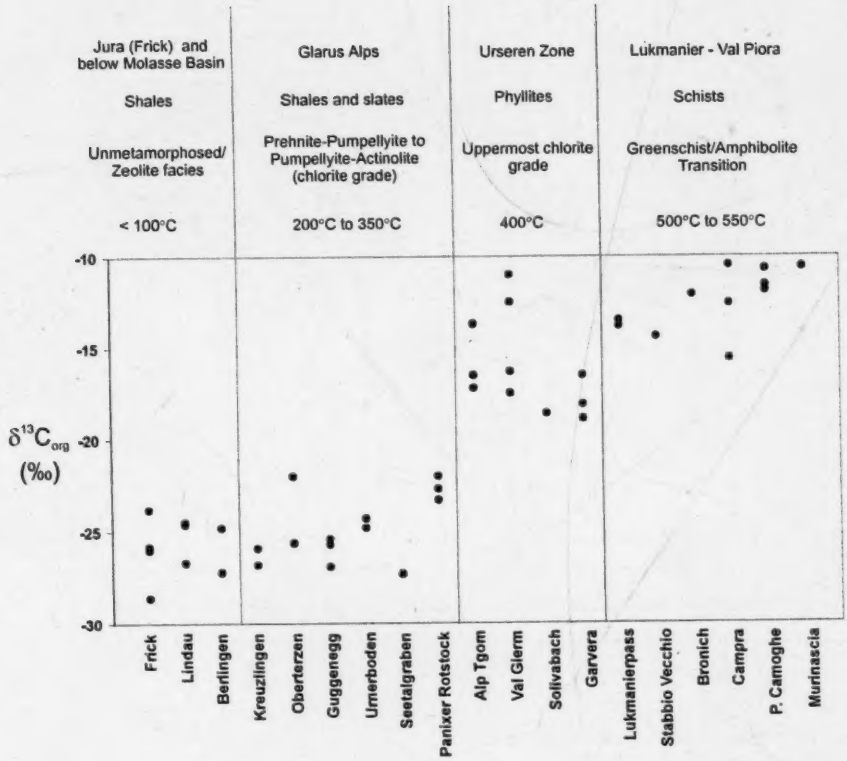

FIGURE 9: $\delta^{13}C_{org}$ isotope profile of the Liassic black shale series (Swiss Alps) showing progressive enrichment in organic carbon isotopic composition during prograde metamorphism. Modified after Hoefs and Frey (1976).

lead to diffusion of Re and Os within ORMs and result in the gain of Re and Os by phases poor in these elements (and vice versa), but it would probably not be systematic enough to preserve the partially reset ~ 471 Ma isochron; a scattered errorchron is more likely. Furthermore, hydrocarbon maturation processes dominate at temperatures corresponding to the oil and gas window (i.e., 50°C-250°C; Stahl, 1974). It has been previously shown that thermal cracking processes do not alter the Re-Os systematics of ORMs during hydrocarbon maturation (the Exshaw Formation; Creaser et al., 2002) or low-chlorite grade metamorphism (the present study). It therefore seems unreasonable to assume that this process could have mobilized Re and/or Os in the UMG slates. Interaction between organic and carbonate carbon is a more likely possibility. However, the general absence of carbonate veins within the UMG slates at the sampling locality suggests this process was not significant. In addition, the UMG slates contain only minor abundances of disseminated carbonate minerals, which themselves contain eight times less carbon than graphite (Valley, 1986). Carbon isotope exchange reactions at low temperatures proceeds by diffusion and is very sluggish (i.e., < ~ 20% at 400°C; Chacko et al., 1991). Exchange of unradiogenic Os from carbonates (which generally contain much lower concentrations of Re and Os compared to ORMs) with radiogenic Os from ORMs is also not likely to be systematic enough to preserve a partially reset isochron. These considerations suggests that carbon isotope exchange between

carbonate and organic matter is not expected to significantly mobilize Re and Os.

What other process might be responsible for disturbing the Re-Os system in the UMG slates? It is interesting to note that at ~ 300°C, organic matter transforms to a higher degree of crystallinity (graphite-d_2-d_1; Landis, 1971). Perhaps the bonds between Re and Os and their host organocomplexes are weakened enough by this process to allow diffusion of Re and Os to take place within the UMG slates. Such diffusion would become more significant with increasing temperature. The question then is whether this process is capable of systematically redistributing Re and Os within the UMG slates in such a way that a partially reset isochron defining an age of ~ 471 Ma can be obtained. The Re-Os systematics of ORMs may also be further altered when graphite becomes fully ordered at ~ 500°C. Further study will be needed to consider these possibilities.

Previous studies suggest that Re may be more mobile than Os during weathering processes (Jaffe et al., 2002; Pierson-Wickmann et al., 2002) and metamorphism (e.g., eclogite- and blueschist-facies; Becker, 2000). In addition, Selby and Creaser (2002) demonstrated that changes in Re complex phases and/or bond types occurred during hydrocarbon maturation of the Exshaw Formation while no evidence for corresponding changes in Os was seen. Partial re-distribution of Re within the UMG slates may therefore have been more important than Os mobilization during middle-chlorite grade metamorphism.

This first look at the response of the Re-Os radioisotope system in ORMs to prograde metamorphism seems to indicate that precise depositional ages may be obtained from these clastic sediments only if they have not been metamorphosed beyond low-chlorite grade. Further understanding of the changes in Re-Os systematics in ORMs during prograde metamorphism can only be obtained by tracing a single, stratigraphically well-constrained ORM horizon over a large range of metamorphic conditions. Furthermore, if changes in the chemistry and structure of various types of hydrocarbons in ORMs during prograde metamorphism are known, they could be directly compared with the corresponding changes in Re-Os systematics. This may shed further insight on the organocomplexes with which Re and Os may be dominantly associated.

CONCLUSIONS

1. Precise ^{187}Re-^{187}Os depositional ages of 620.8 ± 8.1 Ma (MSWD = 0.9; I_{Os} = 0.68 ± 0.06) and 607.6 ± 8.3 Ma (MSWD = 1.4; I_{Os} = 0.63 ± 0.05) were obtained with conventional inverse aqua regia and CrO_3-H_2SO_4 dissolution techniques, respectively, for carbonaceous, sulfidic slates of the OFP from the Windermere Supergroup, southeastern Canadian Cordillera. Both ages are compatible with known absolute age constraints for the Windermere Supergroup.

2. These two precise ages have important implications for future Re-Os dating studies of ORM intervals. For the first time, it was demonstrated that Re and Os remained a closed system during low-chlorite grade metamorphism. Furthermore, it is possible to obtain precise and accurate Re-Os depositional ages from low-TOC (< 1.0%) ORMs. Collection of ORM samples from outcrop does not preclude the ability of the Re-Os system to provide depositional ages, although care must be taken to ensure the analyzed sample material is unweathered.
3. The hydrogenous Re and Os budget of the OFP slates is contaminated by a component of radiogenic detrital Re and Os. Because nearly all the Re and Os associated with organic matter is hydrogenous in origin, the CrO_3-H_2SO_4 digestion method provides the best depositional age determination of the upper OFP carbonaceous interval (607.6 ± 8.3 Ma). The corresponding I_{Os} value of 0.63 ± 0.05 is interpreted to reflect the Os isotopic composition of the contemporaneous seawater at the time of sediment deposition.
4. The depositional age of ~ 608 Ma provides a minimum absolute age constraint on the timing of the second Windermere glaciation which is represented in the Canadian Cordillera by the stratigraphically underlying Mount Vreeland (northeastern British Columbia) and Ice Brook (Mackenzie Mountains) Formations. This glaciation is considered as Lower Marinoan in age and distinct from the Upper

Marinoan (~ 580-570 Ma) glaciogenic deposits of northeastern North America.

5. Further application of the Re-Os geochronometer to other ORMs temporally and spatially related to Neoproterozoic glacial intervals will allow further opportunities for their correlation and provide better age constraints on the timing, duration, and extent of the Neoproterozoic glaciations as well as determine the number of ice ages. This will allow a better assessment of the Snowball Earth theory and its prediction of global, synchronous glaciations.
6. The $^{187}Os/^{188}Os$ isotopic ratio of ~ 0.63 for ~ 608 Ma Neoproterozoic seawater is significantly less radiogenic than that of present-day seawater (~ 1.04-1.07). The most likely explanation for this difference is an increased unradiogenic hydrothermal Os input to the ~ 608 Ma oceans as a result of Laurentian-Rodinian rifting during the Lower Marinoan glaciation.
7. A well-fitted isochron corresponding to an age of 471 ± 11 Ma (MSWD = 1.3) was obtained for the middle-chlorite grade UMG slates. This age is not in agreement with existing absolute age constraints for the UMG (~ 608-570 Ma). Mobilization of Re and Os (possibly as a result of diffusion during organic matter recrystallization) during metamorphism likely occurred along with the thermal alteration of organic matter in the UMG slates. The ~ 471 Ma age is therefore interpreted as a geologically meaningless average of

the true depositional (~ 590 Ma) and metamorphic (~ 100 to 45 Ma) ages. This suggests that the Re-Os geochronometer may not be applicable to ORMs metamorphosed beyond lower-chlorite grade.

REFERENCES

Aalto K. R. (1971) Glacial marine sedimentation and stratigraphy of the Toby Conglomerate (Upper Proterozoic), southeastern British Columbia, northwestern Idaho and northeastern Washington. *Canadian Journal of Earth Sciences* **8**, 753-787.

Aitken J. D. (1991a) The Ice Brook Formation and post-Rapitan Late Proterozoic glaciation, Mackenzie Mountains, Northwest Territories. *Geological Survey of Canada Bulletin 404*, 43 pp.

Aitken J. D. (1991b) Two late Proterozoic glaciations, Mackenzie Mountains, northwestern Canada. *Geology* **19**, 445-448.

Arthur M. A. and Sageman B. B. (1994) Marine black shales: Depositional mechanisms and environments of ancient deposits. *Annu. Rev. Earth Planet. Sci.* **22**, 499-551.

Barfod G. H., Albarède F., Knoll A. H., Xiao S., Télouk P., Frei R., and Baker J. (2002) New Lu-Hf and Pb-Pb age constraints on the earliest animal fossils. *Earth and Planetary Science Letters* **201**, 203-212.

Becker H. (2000) Re-Os fractionation in eclogites and blueschists and the implications for recycling of oceanic crust into the mantle. *Earth and Planetary Science Letters* **177**, 287-300.

Benus A.P. (1988) Sedimentological context of a deep-water Ediacaran fauna (Mistaken Point Formation, Avalon Zone, eastern Newfoundland). In *Trace Fossils, Small Shelly Fossils and the Precambrian-Cambrian Boundary* (eds. E. Landing, G. M. Narbonne, and P. Myrow), pp. 8-9, Bulletin of the New York State Museum.

Birck J. L., Roy Barman M., and Capmas F. (1997) Re-Os isotopic measurements at the femtomole level in natural samples. *Geostandards Newsletter* **20**, 19-27.

Campbell R. B., Mountjoy E. W., and Young F. G. (1973) Geology of the McBride map-area, British Columbia. *Geological Survey of Canada, Paper 72-35*, 104 pp.

Chacko T., Mayeda T. K., Clayton R. N., and Goldsmith J. R. (1991) Oxygen and carbon isotope fractionations between CO_2 and calcite. *Geochimica et Cosmochimica Acta* **55**, 2867-2882.

Charlesworth H. A. K., Weiner J. L., Akehurst A. J., Bielenstein H. U., Evans C. R., Griffiths R. E., Remington D. B., Stauffer M. R., and Steiner J. (1967) Precambrian geology of the Jasper region, Alberta. *Research Council of Alberta Bulletin 23*, 74 pp.

Cohen A. S. and Waters F. G. (1996) Separation of osmium from geological materials by solvent extraction for analysis by thermal ionization mass spectrometry. *Analytica Chimica Acta* **332**, 269-275.

Cohen A. S., Coe A. L., Bartlett J. M., and Hawkesworth C. J. (1999) Precise Re-Os ages of organic-rich mudrocks and the Os isotope composition of Jurassic seawater. *Earth and Planetary Science Letters* **167**, 159-173.

Colpron M., Logan J. M., and Mortensen J. K. (2002) U-Pb zircon age constraint for late Neoproterozoic rifting and initiation of the lower Paleozoic passive margin of western Laurentia. *Canadian Journal of Earth Sciences* **39**, 133-143.

Creaser R. A., Papanastassiou D. A., and Wasserburg G. J. (1991) Negative thermal ion mass spectrometry of osmium, rhenium, and iridium. *Geochimica et Cosmochimica Acta* **55**, 397-401.

Creaser R. A., Sannigrahi P., Chacko T., and Selby D. (2002) Further evaluation of the Re-Os geochronometer in organic-rich sedimentary rocks: A test of hydrocarbon maturation effects in the Exshaw Formation, Western Canada Sedimentary Basin. *Geochimica et Cosmochimica Acta* **66**, 3441-3452.

Crowley T. J., Hyde W. T., and Peltier W. R. (2001) CO_2 levels required for deglaciation of a "Near-Snowball" Earth. *Geophysical Research Letters* **28**, 283-286.

Dempster T. J., Rogers G., Tanner P. W. G., Bluck B. J., Muir R. J., Redwood S. D., Ireland T. R., and Paterson B. A. (2002) Timing of deposition, orogenesis and glaciation within the Dalradian rocks of Scotland: Constraints from U-Pb zircon ages. *Journal of the Geological Society of London* **159**, 83-94.

Esser B. K. and Turekian K. K. (1993) The osmium isotopic composition of the continental crust. *Geochimica et Cosmochimica Acta* **57**, 3093-3104.

Evans D. A. D. (2000) Stratigraphic, geochronological, and paleomagnetic constraints upon the Neoproterozoic climatic paradox. *American Journal of Science* **300**, 347-433.

Gramlich J. W., Murphy T. J., Garner E. L., and Shields W. R. (1973) Absolute isotopic abundance ratio and atomic weight of a reference sample of rhenium. *J. Res. Nat. Bur. Stand.* **77A**, 691-697.

Greenwood H. J., Woodsworth G. J., Read P. B., Ghent E. D., and Evenchick C. A. (1991) Metamorphism, Chapter 16. In *Geology of the Cordilleran Orogen in Canada* (eds. H. Gabrielse and C. J. Yorath), pp. 533-570, Geological Survey of Canada, Geology of Canada, no. 4.

Halverson G. P., Hoffman P. F., Schrag D. P., and Kaufman A. J. (2002) A major perturbation of the carbon cycle before the Ghaub glaciation (Neoproterozoic) in Namibia: Prelude to Snowball Earth? *Geochemistry, Geophysics, Geosystems* **3**, 2001 GC000244.

Hauri E. H. and Hart S. R. (1993) Re-Os isotope systematics of HIMU and EMII oceanic island basalts from the south Pacific Ocean. *Earth and Planetary Sciences* **114**, 353-371.

Hein F. J. and McMechan M. E. (1994) Proterozoic – Lower Cambrian strata of the Western Canada Sedimentary Basin. In *Geological Atlas of the Western Canada Sedimentary Basin* (eds. G. D. Mossop and I. Shetsen), pp. 57-68, Canadian Society of Petroleum Geologists, Calgary, Alberta.

Hoefs J. and Frey M. (1976) The isotopic composition of carbonaceous matter in a metamorphic profile from the Swiss Alps. *Geochimica et Cosmochimica Acta* **40**, 945-951.

Hoffman P. F. and Schrag D. P. (2000) Snowball Earth. *Scientific American* **283**, 68-75.

Hoffman P. F. and Schrag D. P. (2002) The Snowball Earth hypothesis: testing the limits of global change. *Terra Nova* **14**, 129-155.

Hoffman P. F., Kaufman A. J., Halverson G. P., and Schrag D. P. (1998a) A Neoproterozoic Snowball Earth. *Science* **281**, 1342-1346.

Hoffman P. F., Kaufman A. J., and Halverson G. P. (1998b) Comings and goings of global glaciations on a Neoproterozoic tropical platform in Namibia. *GSA Today* **8**, 1-9.

Hyde W. T., Crowley T. J., Baum S. K., and Peltier W. R. (2000) Neoproterozoic 'snowball Earth' simulations with a coupled climate/ice-sheet model. *Nature* **405**, 425-429.

Jaffe L. A., Peucker-Ehrenbrink B., and Petsch S. T. (2002) Mobility of rhenium, platinum group elements and organic carbon during black shale weathering. *Earth and Planetary Science Letters* **198**, 339-353.

James N. P., Narbonne G. M., and Kyser T. K. (2001) Late Neoproterozoic cap carbonates: Mackenzie Mountains, northwestern Canada: Precipitation and global glacial meltdown. *Canadian Journal of Earth Sciences* **38**, 1229-1262.

Kaufman A. J., Knoll A. H., and Narbonne G. M. (1997) Isotopes, ice ages, and terminal Proterozoic Earth history. *Proceedings of the National Academy of Sciences* **94**, 6600-6605.

Kennedy M. J., Runnegar B., Prave A. R., Hoffmann K. -H., and Arthur M. A. (1998) Two or four Neoproterozoic glaciations? *Geology* **26**, 1059-1063.

Kennedy M. J., Christie-Blick N., and Sohl L. E. (2001a) Are Proterozoic cap carbonates and isotopic excursions a record of gas hydrate destabilization following Earth's coldest intervals? *Geology* **29**, 443-446.

Kennedy M. J., Christie-Blick N., and Prave A. R. (2001b) Carbon isotopic composition of Neoproterozoic glacial carbonates as a test of paleoceanographic models for Snowball Earth phenomena. *Geology* **29**, 1135-1138.

Kirschvink J. L. (1992) Late Proterozoic low-latitude global glaciation: The Snowball Earth. In *The Proterozoic Biosphere* (eds. J. W. Schopf and C. Klein), pp. 51-52. Cambridge University Press, New York.

Krogh T. E., Strong D. F., O'Brien S. J., and Papezik V. (1988) Precise U-Pb zircon dates from the Avalon Terrane in Newfoundland. *Canadian Journal of Earth Sciences* **25**, 442-453.

Landis C. A. (1971) Graphitization of dispersed carbonaceous material in metamorphic rocks. *Contributions to Mineralogy and Petrology* **30**, 34-45.

Levasseur S., Birck J.- L., and Allègre C. J. (1998) Direct measurement of femtomoles of osmium and the $^{187}Os/^{186}Os$ ratio in seawater. *Science* **282**, 272-274.

Levasseur S., Birck J.- L., and Allègre C. J. (1999) The osmium riverine flux and the oceanic mass balance of osmium. *Earth and Planetary Science Letters* **174**, 7-23.

Levasseur S., Rachold V., Birck J.- L., and Allègre C. J. (2000) Osmium behavior in estuaries: the Lena River example. *Earth and Planetary Science Letters* **177**, 227-235.

Ludwig K. R. (1998) Isoplot-Ex. Berkeley Geochronology Center.

Martin C. E., Peucker-Ehrenbrink B., Brunskill G. J., and Szymczak, R. (2000) Sources and sinks of unradiogenic osmium runoff from

Papua New Guinea. *Earth and Planetary Science Letters* **183**, 261-274.

McDonough M. R. and Simony P. S. (1986) Geology of the northern Selwyn Range, western Main Ranges, Rocky Mountains, British Columbia: Preliminary report. *Current Research, Part A, Geological Survey of Canada, Paper 86-1A*, 619-626.

McDonough M. R. and Simony P. S. (1988) Stratigraphy and structure of the late Proterozoic Miette Group, northern Selwyn Range, Rocky Mountains, British Columbia. *Current Research, Part D, Geological Survey of Canada, Paper 88-1D*, 105-113.

McKirdy D. M., Sumartojo J., Tucker, D. H., and Gostin V. (1975) Organic, mineralogic and magnetic indications of metamorphism in the Tapley Hill Formation, Adelaide Geosyncline. *Precambrian Research* **2**, 345-373.

McKirdy D. M., Burgess J. M., Lemon N. M., Yu X., Cooper A. M., Gostin V. A., Jenkins R. J. F., and Both R. A. (2001) A chemostratigraphic overview of the late Cryogenian interglacial sequence in the Adelaide Fold-Thrust Belt, South Australia. *Precambrian Research* **106**, 149-186.

McMechan M. E. (1987) Stratigraphy and structure of the Mount Selwyn area, Rocky Mountains, northeastern British Columbia. *Geological Survey of Canada Paper 85-28*, 34 pp.

McMechan M. E. (1990) Upper Proterozoic to Middle Cambrian history of the Peace River Arch: Evidence from the Rocky Mountains. *Bulletin of Canadian Petroleum Geology* **38A,** 36-44.

McMechan M. E. (2000) Vreeland diamictites – Neoproterozoic glaciogenic slope deposits, Rocky Mountains, northeast British Columbia. *Bulletin of Canadian Petroleum Geology* **48**, 246-261.

McMechan M. E. and Thompson R. I. (1995) Geology and structure section, Ovington Creek, British Columbia. *Geological Survey of Canada Map 1873A*, scale 1:50 000.

Meisel T., Walker R. J., and Morgan J. W. (1996) The osmium isotopic composition of the Earth's primitive upper mantle. *Nature* **383**, 517-520.

Monger J. W. H. and Price R. A. (1979) Geodynamic evolution of the Canadian Cordillera – Progress and problems. *Canadian Journal of Earth Sciences* **16**, 770-791.

Monger J. W. H., Price R. A., and Tempelman-Kluit D. J. (1982) Tectonic accretion and the origin of the two major metamorphic and plutonic belts in the Canadian Cordillera. *Geology* **10**, 70-75.

Morgan J. W., Golightly D. W., and Dorrzapf A. F. Jr. (1991) Methods for the separation of rhenium, osmium and molybdenum applicable to isotope geochemistry. *Talanta* **38**, 259-265.

Morgan J. W., Horan M. F., Walker R. J., and Grossman J. N. (1995) Rhenium-osmium concentrations and isotope systematics in group

IIAB iron meteorites. *Geochimica et Cosmochimica Acta* **59**, 2331-2344.

Narbonne G. M., Kaufman A. J., and Knoll A. H. (1994) Integrated chemostratigraphy and biostratigraphy of the Windermere Supergroup, northwestern Canada: Implications for Neoproterozoic correlations and the early evolution of animals. *Geological Society of America Bulletin* **106**, 1281-1292.

Oxburgh R. (1998) Variations in the osmium isotope composition of sea water over the past 200,000 years. *Earth and Planetary Science Letters* **159**, 183-191.

Oxburgh R. (2001) Residence time of osmium in the oceans. *Geochemistry, Geophysics, Geosystems* **2**, 2000GC000104.

Palmer M. R., Falkner K. K., Turekian K. K., and Calvert S. E. (1988) Sources of osmium isotopes in manganese nodules. *Geochimica et Cosmochimica Acta* **52**, 1197-1202.

Pavlov A. A., Kasting J. F., Brown L. L., Rages K. A., and Freedman R. (2000) Greenhouse warming by CH_4 in the atmosphere of early Earth. *Journal of Geophysical Research* **105**, 11,981-11,990.

Pegram W. J., Esser B. K., Krishnaswami S., and Turekian K. K. (1994) The isotopic composition of leachable osmium from river sediments. *Earth and Planetary Science Letters* **128**, 591-599.

Pell J. and Simony P. S. (1987) New correlations of Hadrynian strata, south-central British Columbia. *Canadian Journal of Earth Sciences* **24**, 302-313.

Peucker-Ehrenbrink B. and Ravizza G. (1996) Continental runoff of osmium into the Baltic Sea. *Geology* **24**, 327-330.

Peucker-Ehrenbrink B. and Blum J. D. (1998) Re-Os isotope systematics and weathering of Precambrian crustal rocks: Implications for the marine osmium isotope record. *Geochimica et Cosmochimica Acta* **62**, 3193-3203.

Peucker-Ehrenbrink B. and Hannigan R. E. (2000) Effects of black shale weathering on the mobility of rhenium and platinum group elements. *Geology* **28**, 475-478.

Pierson-Wickmann A.-C., Reisberg L., and France-Lanord C. (2000) The Os isotopic composition of Himalayan river bedloads and bedrocks: Importance of black shales. *Earth and Planetary Science Letters* **176**, 203-218.

Pierson-Wickmann A.-C., Reisberg L., and France-Lanord C. (2002) Behavior of Re and Os during low-temperature alteration: Results from Himalayan soils and altered black shales. *Geochimica et Cosmochimica Acta* **66**, 1539-1548.

Prave A. R. (1999) Two diamictites, two cap carbonates, two $\delta^{13}C$ excursions, two rifts: The Neoproterozoic Kingston Peak Formation, Death Valley, California. *Geology* **27**, 339-342.

Price R. A. (1994) Cordilleran tectonics and the evolution of the Western Canada Sedimentary Basin. In *Geological Atlas of the Western Canada Sedimentary Basin* (eds. G. D. Mossop and I. Shetsen), pp. ??, Canadian Society of Petroleum Geologists, Calgary, Alberta.

Ravizza G. and Turekian K. K. (1989) Application of the ^{187}Re-^{187}Os system to black shale geochronometry. *Geochimica et Cosmochimica Acta* **53**, 3257-3262.

Ravizza G. and Turekian K. K. (1992) The osmium isotopic composition of organic-rich marine sediments. *Earth and Planetary Science Letters* **110**, 1-6.

Ravizza G. and Esser B. K. (1993) A possible link between the seawater osmium isotope record and weathering of ancient sedimentary organic matter. *Chemical Geology* **107**, 255-258.

Ravizza G., Turekian K. K., and Hay B. J. (1991) The geochemistry of rhenium and osmium in recent sediments from the Black Sea. *Geochimica et Cosmochimica Acta* **55**, 3741-3752.

Reisberg L., Zindler A., Marcantonio F., White W., Wyman D., and Weaver B. (1993) Os isotope systematics in ocean island basalts. *Earth and Planetary Science Letters* **120**, 149-167.

Ripley E. M., Park Y.-R., Lambert D. D., and Frick L. R. (2001a) Re-Os isotopic variations in carbonaceous pelites hosting the Duluth Complex: Implications for metamorphic and metasomatic processes

associated with mafic magma chambers. *Geochimica et Cosmochimica Acta* **65**, 2965-2978.

Ripley E. M., Park Y.-R., Lambert D. D., and Frick L. R. (2001b) Re-Os isotopic composition and PGE contents of Proterozoic carbonaceous argillites, Virginia Formation, northeastern Minnesota. *Organic Geochemistry* **32**, 857-866.

Ross G. M. (1991a) Meltdown of the second Windermere glaciation: A working hypothesis [abstract]. *Geological Association of Canada Abstracts With Programs* **16**, A107.

Ross G. M. (1991b) Tectonic setting of the Windermere Supergroup revisited. *Geology* **19**, 1125-1128.

Ross G. M. and Murphy D. C. (1988) Transgressive stratigraphy, anoxia, and regional correlations within the late Precambrian Windermere grit of the southern Canadian Cordillera. *Geology* **16**, 139-143.

Ross G. M. and Villeneuve M. E. (1997) U-Pb geochronology of stranger stones in Neoproterozoic diamictites, Canadian Cordillera: Implications for provenance and ages of deposition. In *Radiogenic Age and Isotopic Studies: Report 10*, Geological Survey of Canada Current Research 1997-F.

Ross G. M., McMechan M. E., and Hein F. J. (1989) Proterozoic history: Birth of the miogeocline. In *The Western Canada Sedimentary Basin* (ed. B. D. Ricketts), pp. 79-104, Canadian Society of Petroleum Geologists, Calgary, Alberta.

Ross G. M., Bloch J. D., and Krouse H. R. (1995) Neoproterozoic strata of the southern Canadian Cordillera and the isotopic evolution of seawater sulfate. *Precambrian Research* **73**, 71-99.

Schaefer B. F. and Burgess J. M. (2001) Re-Os isotopic age constraints on deposition in the Neoproterozoic Amadeus Basin: Implications for the "Snowball Earth" [abstract]. *EOS; Trans. Am. Geophys. Union* **82**, F770.

Schrag D. P., Berner R. A., and Hoffman P. F. (2002) On the initiation of a Snowball Earth. *Geochemistry, Geophysics, Geosystems* **3**, 2001 GC000219.

Selby D. and Creaser R. A. (2001) Re-Os geochronology and systematics in molybdenite from the Endako porphyry molybdenum deposit, British Columbia, Canada. *Economic Geology* **96**, 197-204.

Selby D. and Creaser R. A. (2002) Analytical considerations for Re-Os analysis of organic-rich sediments: Implications for accurate and precise Re-Os dates. *Geochimica et Cosmochimica Acta* (in review).

Sharma M. and Wasserburg G. J. (1997) Osmium in the rivers. *Geochimica et Cosmochimica Acta* **61**, 5411-5416.

Sharma M., Papanastassiou D. A., and Wasserburg G. J. (1997) The concentration of isotopic composition of osmium in the oceans. *Geochimica et Cosmochimica Acta* **61**, 3287-3299.

Sharma M., Wasserburg G. J., Hofmann A. W., and Butterfield D. A. (2000) Osmium isotopes in hydrothermal fluids from the Juan de Fuca Ridge. *Earth and Planetary Science Letters* **179**, 139-152.

Shirey S. B. and Walker R. J. (1995) Carius tube digestion for low-blank rhenium-osmium analysis. *Analytical Chemistry* **67**, 2136-2141.

Singh S. K., Trivedi J. R., and Krishnaswami S. (1999) Re-Os isotope systematics in black shales from the Lesser Himalaya: Their chronology and role in the $^{187}Os/^{188}Os$ evolution of seawater. *Geochimica et Cosmochimica* Acta **63**, 2381-2392.

Smoliar M. I., Walker R. J., and Morgan J. W. (1996) Re-Os ages of Group IIA, IIIA, IVA, and IVB iron meteorites. *Nature* **271**, 1099-1102.

Stahl W. (1971) Carbon isotope fractionations in natural gases. *Nature* **251**, 134-135.

Thompson M. D. and Bowring S. A. (2000) Age of the Squantum 'tillite', Boston Basin, Massachusetts: U-Pb zircon constraints on terminal Neoproterozoic glaciation. *American Journal of Science* **300**, 630-655.

Valley J. W. (1986) Stable isotope geochemistry of metamorphic rocks. In *Stable Isotopes in High Temperature Geological Processes* (Eds. J. W. Valley, H. P. Taylor Jr., and J. R. O'Neil), pp. 445-489, Mineralogical Society of America, Reviews in Mineralogy, Volume 16.

Valley J. W. and O'Neil J. R. (1981) $^{13}C/^{12}C$ exchange between calcite and graphite: A possible thermometer in Grenville marbles. *Geochimica et Cosmochimica Acta* **45**, 411-419.

Völkening J., Walczyk T., and Heumann K. G. (1991) Osmium isotope ratio determinations by negative thermal ionization mass spectrometry. *International Journal of Mass Spectrometry and Ion Processes* **105**, 147-159.

Walker R. J., Shirey S. B., and Stecher O. (1988) Comparative Re-Os, Sm-Nd, and Rb-Sr isotope and trace element systematics for Archean komatiite flows from Munro Township, Abitibi Belt, Ontario. *Earth and Planetary Science Letters* **87**, 1-12.

Walker R. J., Prichard H. M., Ishiwatari A., and Pimentel M. (2002) The osmium isotopic composition of convecting upper mantle deduced from ophiolite chromites. *Geochimica et Cosmochimica Acta* **66**, 329-345.

Walter M. R., Veevers J. J., Calver C. R., Gorjan P., and Hill A. C. (2000) Dating the 840-544 Ma Neoproterozoic interval by isotopes of strontium, carbon, and sulphur in seawater, and some interpretative models. *Precambrian Research* **100**, 371-433.

Williams D. M., Kasting J. F., and Frakes L. A. (1998) Low-latitude glaciation and rapid changes in the Earth's obliquity explained by obliquity-oblateness feedback. *Nature* **396**, 453-455.

Williams G. E. (1975) Late Precambrian glacial climate and the Earth's obliquity. *Geological Magazine* **112**, 441-544.

Williams G. E. (1993) History of the Earth's obliquity. *Earth-Science Reviews* **34**, 1-45.

Williams G. E. (1998) Precambrian tidal and glacial clastic deposits: Implications for Precambrian Earth-Moon dynamics and palaeoclimate. *Sedimentary Geology* **120**, 55-74.

Williams G. and Schmidt P. (2000) Proterozoic equatorial glaciation: Has 'Snowball Earth' a snowball's chance? *The Australian Geologist* **117**, 21-25.

Woodhouse O. B., Ravizza G., Falkner K. K., Statham P. J., and Peucker-Ehrenbrink B. (1999) Osmium in seawater: Vertical profiles of concentration and isotopic composition in the eastern Pacific Ocean. *Earth and Planetary Science Letters* **173**, 223-233.

Young G. M. (1976) Iron formation and glaciogenic rocks of the Rapitan Group, Mackenzie Mountains, Yukon and Northwest Territories, Canada. *Precambrian Research* **3**, 137-158.

APPENDIX ONE: SAMPLE DETAILS

Samples*	Lithology	Location
UPPER MIETTE GROUP, WINDERMERE SUPERGROUP (6) BK-01-009 BK-01-010 BK-01-011 BK-01-012 BK-01-013A BK-01-013B	Black carbonaceous, sulfidic slates from a roadcut along Highway 16	Mount Robson, B.C. (74 km west of Jasper, Alberta) 53°01.715′ N 119°10.141′ W
OLD FORT POINT FORMATION, WINDERMERE SUPERGROUP (6) BK-01-014A BK-01-014B BK-01-015A BK-01-015B BK-01-015C BK-01-015D	Dark grey carbonaceous, sulfidic slates from a roadcut along Highway 16	Geikie-Siding, Alberta (14 km west of Jasper, Alberta) 52°52.346′ N 118°17.722′ W

* Stratigraphic interval of sampling is 50 cm for both Upper Miette Group and Old Fort Point Formation slates.